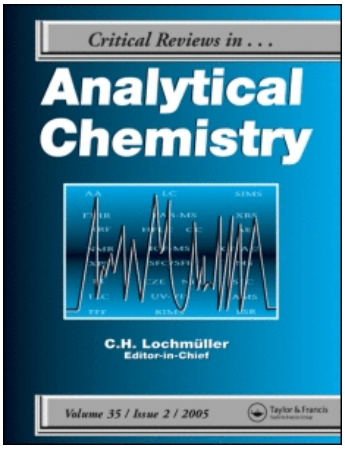

Critical Reviews in Analytical Chemistry
Publication details, including instructions for authors and subscription information:
http://www.informaworld.com/smpp/title~content=t713400837

Background Correction in Atomic Absorption Spectroscopy (AAS)

Walter Slavin; Glen R. Carnrick; S. Roy Koirtyohann

To cite this Article Slavin, Walter , Carnrick, Glen R. and Koirtyohann, S. Roy(1988) 'Background Correction in Atomic Absorption Spectroscopy (AAS)', Critical Reviews in Analytical Chemistry, 19: 2, 95 — 134
To link to this Article: DOI: 10.1080/10408348808542809
URL: http://dx.doi.org/10.1080/10408348808542809

BACKGROUND CORRECTION IN ATOMIC ABSORPTION SPECTROSCOPY (AAS)

Authors: **Walter Slavin**
Glen R. Carnrick
Perkin-Elmer Corporation
Ridgefield, Connecticut

Referee: S. Roy Koirtyohann
Department of Chemistry
University of Missouri
Columbia, Missouri

I. HISTORICAL INTRODUCTION

Atomic absorption spectroscopy (AAS) is fundamentally a very simple technique. Light at the resonance wavelength of an element can be absorbed by atoms of that element in the vapor phase. This reduction in light from the source is the AAS signal. It is monotonically correlated with the number of atoms through which the light must pass. If anything else in the sample (the matrix) can reduce the intensity of radiation from the source, by scattering or molecular absorption, it will be indistinguishable from the analyte. This nonanalyte signal is called background absorption in this article whether the cause of the signal is scattering or absorption.

In flame AAS, the sample is converted into an atomic vapor by burning in a high temperature flame. The short residence time of material in the flame keeps the effects due to the matrix small and, for a long time, background absorption was not reported. The flame AAS book, published in 1968[1], 10 years after the first flame AAS applications papers, devoted only a page to "light scattering" interferences, first reported in 1962 by Willis.[2] Willis showed that loss of analytical radiation by scattering from particles in the flame or by absorption of molecules that were not dissociated in the flame caused errors that could not be corrected by the method of additions. He used nearby lines in the light source to correct for the interference. Koirtyohann and several colleagues studied the effect and decided that in many situations the signal loss was due to molecular absorption and not to scattering. In 1965, he and Pickett[3] used a continuum source to make a simultaneous measurement which, when subtracted from the signal from the element source, yielded a background-corrected AAS signal.

However, others were looking for better ways to correct for background; in 1966 and 1967 Ling[4] in Australia and Barringer[5] in Canada proposed that better correction was obtained by using radiation closer to the resonance line by self-absorbing the center of a broadened resonance line and using the wings for correction. Their idea was extended by Baranov et al.[6] and later by Smith and Hieftje[7] to a wider range of elements by providing a high current pulse to a conventional hollow cathode lamp (HCL). The broadened resonance line will be self-absorbed by the metal vapor in front of the cathode to provide background correction only slightly removed from the absorption line.

Background correction in flame AAS was not a serious problem. When it was observed at all, the effect was small and was easily corrected. With the advent of the graphite furnace, however, backgrounds were large and background correction was mandatory for accurate results. The furnace was invented by a Russian physicist, L'vov,[8] in 1959, but the first paper accessible to Western workers was published in 1961.[9] The furnace seemed promising but was difficult to use. In 1968, Massmann[10] published a simplification of the L'vov furnace

and a commercial furnace was introduced in 1969 based on Massmann's design. The commercial furnace instrument used the then commercial continuum background corrector of Koirtyohann and Pickett.[3] It soon became apparent that furnace AAS produced significant, and frequently large, background absorption from matrix materials that were not decomposed to the atomic state. This background absorption had to be corrected if results were to be accurate.

At about the same time, in 1969, Prügger and Torge[11] and Hadeishi and McLaughlin[12] independently considered the Zeeman effect for furnace AAS. Zeeman effect background correction has emerged as the most effective way to correct for background problems in graphite furnace AAS.

In his initial publication in 1955, Walsh[13] showed that his use of an elemental light source in conjunction with a simple monochromator of low dispersion provided spectral resolution equivalent to the atomic linewidth of the source. Nevertheless, in 1965 Fassel et al.[14] showed that AAS could be usefully performed with a continuum source and a monochromator with resolution better than that required by the Walsh arrangement. This idea was later picked up again for simultaneous multielement AAS analyses and extensively developed by O'Haver and colleagues.[15]

Using Fassel's continuum system, Snelleman[16] showed in 1968 that molecular absorption or scattering was corrected by modulating the source wavelength over a small wavelength range around the resonance line. In the same year, Svoboda[17] modulated the continuum source wavelength for background correction by using an interference filter in a rotationally oscillatory manner, really a Fabry-Perot interferometer.

Thus, by the end of the 1960s, the stage was set for intense work on background correction for furnace AAS. The need was acute and there were several ideas already in the literature. The use of a nearby wavelength in the source had been replaced by the commercial availability of continuum background correction using a hydrogen or deuterium arc.[3] Alternatively, background was corrected by broadening the source line by increasing the intensity and absorbing the center of the line by self-absorption.[4,5] Others were already obtaining background-corrected AAS signals using a continuum source and modulating the wavelength near the resonance line. Torge, coinventor with Prügger of Zeeman AAS background correction, started well before 1971[18] with experiments using a tunable dye laser source for AA background correction.

While Prügger and Torge[11] and Hadeishi and McLaughlin[12] in 1969 are usually credited with independently applying the Zeeman effect to AAS, others conceived the idea independently. In 1968, Schrenk et al.[19] used the Zeeman effect on a HCL to broaden the spectral line for use in AAS. The Zeeman effect had been extensively studied by physicists for decades. It was well known that when an atomic vapor was excited to emission in a magnetic field the emitted lines were split and moved to slightly different wavelengths.

With the continued focus upon the light source in all the previous AA background correction work, it is not surprising that Prügger and Hadeishi both applied the magnetic field to the light source. The paper of Hadeishi and McLaughlin[12] is very instructive in the logical sequence of their work. They proceeded from the paper of Ling[4] to find a way to correct even closer to the resonance line. Hadeishi referenced the well-known Zeeman technique using a magnetic field to move a line by small, controlled distances. He used a magneto-optical source scanning method that had been published in 1962.[20] He quoted several physics papers from the laboratory of Alkemade, the coinventor of AAS.[21]

While Prügger and Hadeishi are credited with first applying the Zeeman effect to analytical AAS, the physicists had already done the technical things that were required. *High Resolution Spectroscopy* is a classic textbook in atomic spectroscopy by Tolansky[22] published in 1947. He discussed prior literature using the Zeeman effect to split the lines emitted from a HCL. Tolansky also discussed using the Zeeman effect in absorption. Even closer to the point are

the two patents in 1963 of Isaak,[23] a physicist working at the time in Australia. He started with the Walsh AAS patent and pointed out that use of a magnetic field across either a source or an absorbing atomic vapor could be used to alter the spectral width and position of atomic lines used for various physics experiments.

A practical problem impeded these early Zeeman experiments using the magnetic field on the light source. The magnetic field disrupted the performance of hollow cathode light sources and had a significant effect on electrodeless discharge lamps (EDLs), too, which became commercially available in the mid-1970s.[24] Hitachi Corp. introduced a commercial Zeeman instrument in 1974[25] using the Hadeishi design with the magnetic field on the source. Stephens at Dalhousie University in Canada started Zeeman experiments in 1973 with the magnetic field on the source.[26] Both Hitachi Corp. and Stephens continued to report source problems as a result of the magnetic field, although both claimed progress in this situation.

Pearl, working at Varian Techtron in Australia, started in 1971 to use the Zeeman effect for AAS and immediately recognized that the field could be used either on the source or on the analyte. This yielded a patent in 1975.[27] At about the same time, the early 1970s, Woodriff at the University of Montana also independently started using the Zeeman effect for the graphite furnace. Strangely, this work has never been published in the technical literature, but the thesis of Held, a student of Woodriff, from 1972[28] provides documentation of some of the work. Held was discouraged from using the Zeeman effect on the source by his observation that the sources varied in intensity in the magnetic field, especially in an AC magnetic field. Since he was methodically considering the Zeeman effect for background correction, he easily made the transition to the analyte. Although Held's thesis emphasized several "firsts", the magnetic field on the analyte is not so identified because for him the extension was obvious.

Finally, in 1975 and 1976, many workers recognized independently that the magnetic field could be more easily applied to the analyte. The Parker and Pearl patent[27] appeared. The first publication to use the magnetic field on the analyte (a flame) was by Uchida and Hattori[29] in a Japanese journal. Dawson et al.[30] published good Zeeman results in 1977 and Koizumi and Yasuda[31] described a Zeeman AA instrument using a DC permanent magnet on the furnace. Hitachi Corp. introduced their commercial instrument at the FACSS meeting in November 1976.

de Galan appears to be yet another person who independently realized the opportunity of using the magnetic field on the analyte. In a paper[32] devoted to problems associated with conventional continuum background correction, he referenced the Hitachi Zeeman papers using the magnetic field on the source. The de Galan paper was received by the journal in July 1976 just before the Hitachi paper[31] describing the magnetic field on the analyte and just before the Dawson paper. The de Galan paper clearly indicated the belief that they were proposing an idea not yet proposed in the AAS literature where, on page 265, they say: "It would seem possible to remove the coincidence of two absorbing lines by applying the magnetic field to the absorbing vapor." de Galan and de Loos-Vollebregt went on to publish the first comprehensive Zeeman AAS theory in 1978[33] and a series of subsequent papers.

Several long reviews discuss background correction.[34-36] Reviews by de Loos-Vollebregt and de Galan[37] and by Yasuda et al.[38] discuss Zeeman correction in AAS in technical detail. In this monograph, we first discuss the technical issues associated with the several background correction systems, then the need for correction and the potential errors associated with each system. We conclude with a comparison between the systems in which we discuss the advantages and disadvantages of each, especially for future instrumentation.

This review considers background correction for both flame and furnace AAS. As we document in many places in this review, background correction is vastly more important for furnace AAS. Therefore, more attention has been paid to furnace work in this paper. Also, it is the authors' considered opinion that all suppliers of furnace AAS instruments

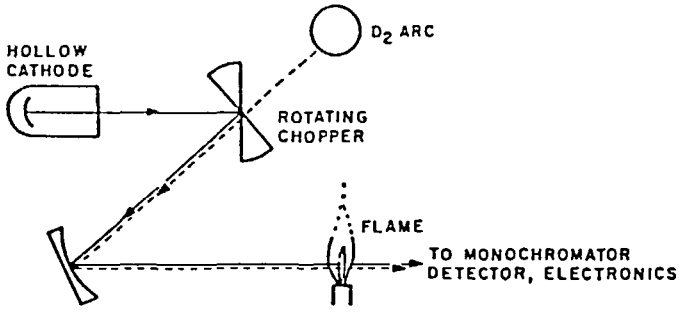

FIGURE 1. Background correction using the continuum (D_2 arc) source. (From Kahn, H. L., *At. Absorpt. Newsl.*, 7, 40, 1968. With permission.)

will use Zeeman correction within the next several years. The emphasis on Zeeman background correction for furnace AAS is thus a reflection of our opinion that this is the issue of greatest analytical importance.

II. CONTINUUM CORRECTION

Continuum correction devices are the most widely used for AAS instrumentation. They depend upon the fact that line sources for atomic absorption, HCLs, and EDLs have extremely narrow linewidths, on the order of 0.003 nm. A second lamp is used which provides a spectrum which is continuous in that it has radiation across the major part of the spectrum used for AAS. A typical optical system is shown in Figure 1 from the paper by Kahn[39] which was based upon the work of Koirtyohann and Pickett.[3] A flame is shown as the device that generates the atomic vapor, but a furnace is just as appropriate. The line source, shown as an HCL, is reflected from a rotating, bladed mirror through the flame, the monochromator, and to the detector. A second light source, shown as a deuterium arc, provides continuous radiation through the same optical system. When the mirror segment is in a position to reflect the HCL radiation, it obstructs radiation from the deuterium lamp. When the open portion of the bladed mirror is on the optical axis, only the continuum radiation is transmitted to the detector. Thus, two signals are generated in rapid sequence.

By reference to Figure 2, the role of the two signals can be understood. Light from the HCL is absorbed by the analyte in the vapor phase because the HCL linewidth is narrower than the absorption linewidth of the analyte. However, the linewidth of the continuum radiation is controlled by the setting of the monochromator, typically somewhat more or less than 1 nm. The absorption of the analyte is negligible in such a broad band so the continuum signal ignores the analyte absorption. Continuum absorption from broad molecular bands or light scattered in the flame or furnace is equally measured by the HCL and continuum lamp. The difference between these two signals is the analyte absorption alone.

Analytical error arising from molecular gases or light scatter is typically corrected effectively in this way and continuum correction has been very valuable for flame AAS. The deuterium arc lamp has an intense continuum in the UV, but it is much less intense in the visible and near infrared. For this reason, many instruments are fitted with both a deuterium arc and a tungsten lamp so that the tungsten thermal continuum can be used for the longer wavelength determinations. In some instruments, the deuterium continuum is produced by filling an HCL with deuterium to save the expense of a different lamp mount and power supply. But the continuum intensity of the deuterium-filled HCL is very low, usually less than 10% of that of the deuterium arc, and an arc should be used.

If there is structure within the absorption band over the spectral width set by the mon-

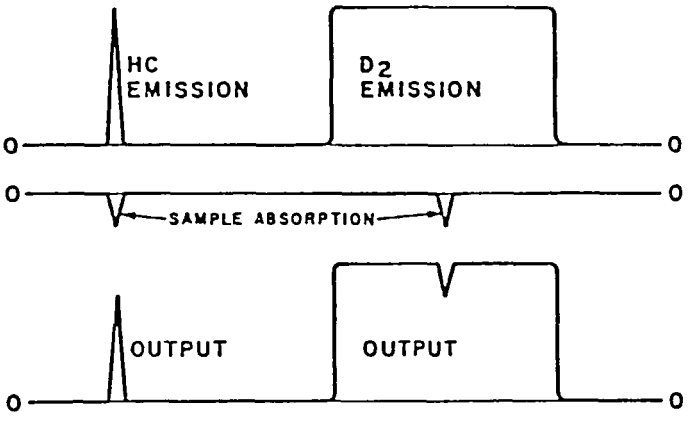

FIGURE 2. Operation of continuum source background correction. The upper panel represents the sequence of emission from the hollow cathode lamp (HC) and the continuum (D_2) lamp. The center panel shows the effect of analyte absorption on both emission signals. The lower panel shows that analyte absorption has a negligible effect on the continuum emission. (From Kahn, H. L., *At. Absorpt. Newsl.*, 7, 40, 1968. With permission.)

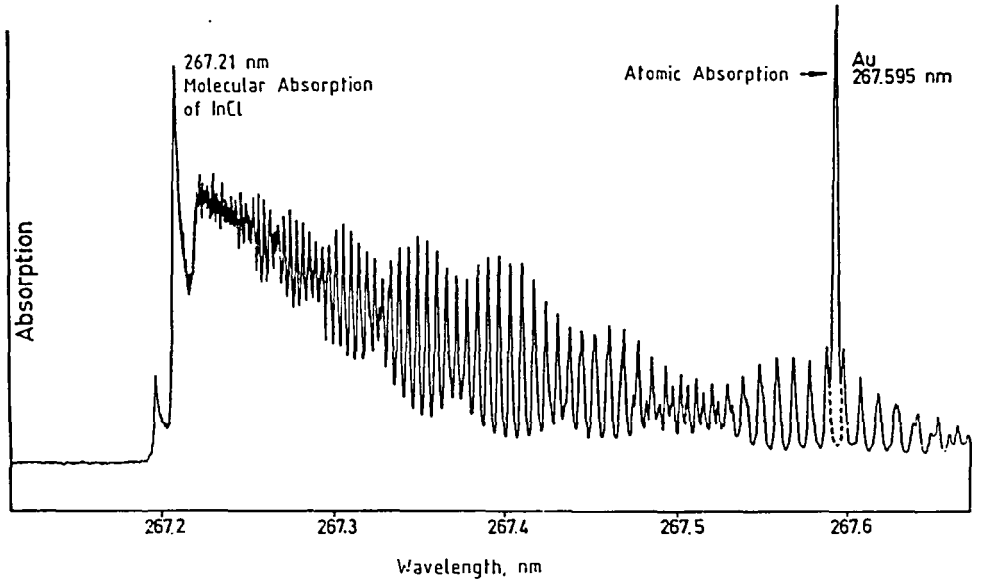

FIGURE 3. The high resolution absorption spectrum of InCl in the neighborhood of the Au resonance line at 267.6 nm. The spectrum is by Massmann,[40] reproduced in Welz.[35]

ochromator, the continuum detector will average the absorption and, often, an error will be introduced. The most common is the presence of an absorption line of a matrix material present at a very high concentration. This matrix absorber will remove radiation from the continuum source, but it is usually far enough from the analyte line not to affect the HCL signal. In this case, the difference signal will have been overcorrected and the analytical result will be too small. In the absence of analyte, this situation will produce an analytical signal that goes below the zero axis.

Also, some compounds in the sample matrix form gaseous molecules that have very narrow absorption bands. An example of this is shown in Figure 3, from Massmann,[40] of

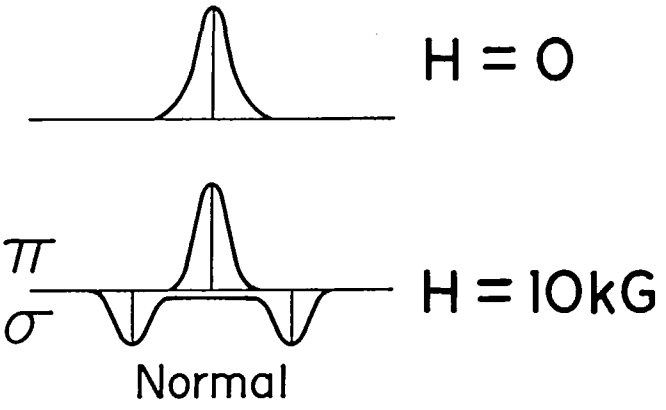

FIGURE 4. Diagram of a normal Zeeman line at zero magnetic field H = 0, and at 10 kG.

the lines formed by InCl near the Au resonance line at 267.6 nm. Clearly, even a 0.2-nm monochromator slit width will include many bands and the average background is unlikely to provide accurate correction. Such an error could be either positive or negative and is often difficult to detect.

Very many continuum background correction errors have been identified in the literature, especially in furnace AAS. It is also necessary to match quite closely the two sources with respect to intensity, beam geometry, and optical path. Since the atomic vapor in both the flame and the furnace is not truly homogeneous, nor is the radiant cross section of either source, this matching is difficult. These problems will be dealt with in a later section.

III. ZEEMAN CORRECTION

Usually, a single isotope of an element will emit a single specific wavelength as the atom returns from an excited to a ground-state energy level. In this situation, the radiation from the atom is unpolarized. Just prior to 1900, Zeeman discovered that in an intense magnetic field the energy levels in the atom are altered slightly. In the simplest case, called a "normal Zeeman pattern" in Figure 4, the line is split so that one component at the original wavelength, polarized in the plane of the magnetic field, contains half the original intensity. Two components, each with one quarter of the original intensity, are polarized in a plane perpendicular to the magnetic field, and each component is displaced an equal distance from the original wavelength.

Those components polarized in the plane of the magnetic field are called "pi" or "π" components and those polarized perpendicular to that plane are called "sigma" or "σ" components. The separation of the two sigma components from the original line is proportional to the magnetic field applied across the atomic vapor. We use the convention that light polarized in the plane parallel to the magnetic field (pi component) is shown above the line, upwards. The radiation polarized orthogonal to the magnetic field (sigma components) is shown below the line, downwards.

The normal Zeeman effect, producing a single pi component at the original wavelength and two sigma components symmetrically displaced from that wavelength, applies to the alkaline earth elements and Cd and Zn of the transitions usually used for AA analysis. Most of the other transitions usually used for AAS display a more complex splitting pattern in which either or both the pi and sigma components are themselves further split (Figure 5). These more complex splitting patterns were not initially understood and were called the

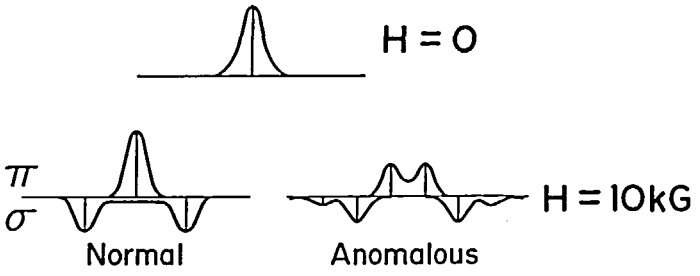

FIGURE 5. Comparison of the splitting of normal and anomalous Zeeman lines at magnetic fields of 0 and 10 kG.

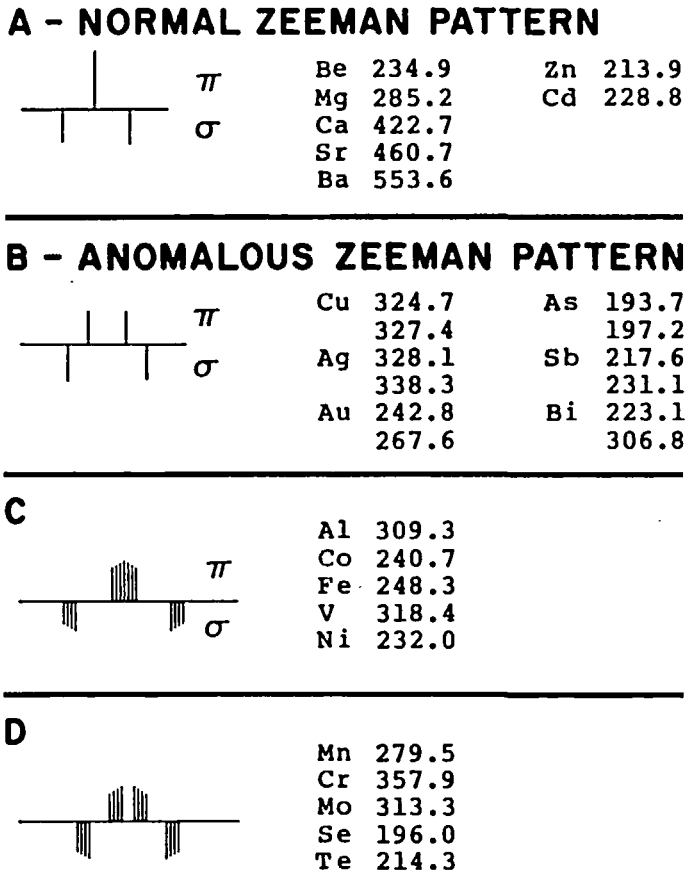

FIGURE 6. Various classes of Zeeman splitting patterns. (Redrawn from Reference 38.)

"anomalous" Zeeman effect. Eventually, they were explained by quantum mechanical theory.

The several categories of splitting are illustrated in Figure 6. Some of the analyte transitions represented by each pattern are also shown. In panel A, several elements with normal Zeeman transitions are shown. Panels B, C, and D represent some typical anomalous Zeeman patterns. In panel B, the pi polarization is also split in two and is displaced from the original line. In panel C, the pi polarization is split into many closely spaced lines and so is each sigma component. In panel D, the pi component is first split in two and then further split.

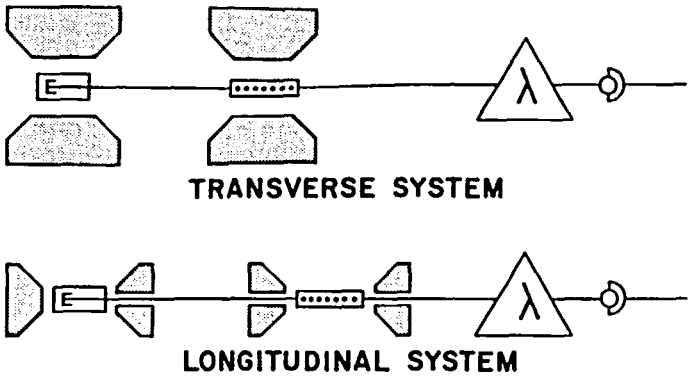

FIGURE 7. Various optical configurations for applying Zeeman background correction. The magnetic field is perpendicular to the optical axis in the transverse system and parallel to the axis in the longitudinal system. The magnet can be applied to the source or to the sampling device, a flame, or furnace.

Instrumentally, the Zeeman effect may be applied in a variety of ways; these are illustrated in Figure 7. The magnet may be aligned so that the magnetic field is perpendicular to the optical axis, which we call the "transverse system". The magnetic field may be applied to the source, i.e., to the atoms that are excited in the lamp. It may also be applied to the analyte atoms in the sample, to the flame, or to the furnace. If the magnetic field is applied to the analyte, the absorption lines are shifted and polarized relative to the source wavelength. The magnet may also be aligned so that the magnetic field is parallel to the optical axis, which we call the "longitudinal system". If a traditional magnet is used for the longitudinal system, holes must be bored through the pole faces to let the light beam pass through.

Another important instrumental variable is that the magnet may be constant, either a permanent magnet or a DC electromagnet, or the electromagnet may be AC. We discuss further and compare the several options utilizing the transverse system, both on the source and on the analyte, including the choice between AC and DC magnet options.

When the DC magnetic field is used on the source and the transition has a normal Zeeman pattern (Figure 8), the source radiation is split into a pi component still at the center of the absorption band and two sigma components symmetrically displaced on either side of the absorption line. In this and the following figures, the following symbols are used. Small k is the absorption coefficient in the furnace. The superscript "a" is the atomic absorption and "b" is the background absorption. The intensity of the source is I and the subscripts π and σ represent the splitting of the source radiation into three wavelengths, at λ_a where the atoms absorb, and λ_1 and λ_2 where background is corrected. The I signal at λ_a measures the sum of $k^a + k^b$ absorption. In that part of the cycle when the two I signals are measured, only k^b is determined and the difference is the signal due to k^a_π.

To separate the pi and sigma components, advantage is taken of their difference in polarization using a prism that imparts an angular separation between the two polarized beams. At least one of the early workers, Dawson (see Reference 30), used two detectors to monitor the two separated beams. However, most instruments use a rotating polarizer that transmits light of one polarization and traps light of the orthogonal polarization. As this polarizer rotates, the pi and sigma components are successively transmitted and alternately fall on the detector.

When the DC magnet is used on the analyte (Figure 9), the absorption profile is split and the signals resulting from the two planes of polarization are separated with a rotating polarizer, as before. Now, with the DC magnetic field on the analyte, it is the absorbance of the analyte, k^a, that is split and measured successively. In the pi part of the cycle, the intensity,

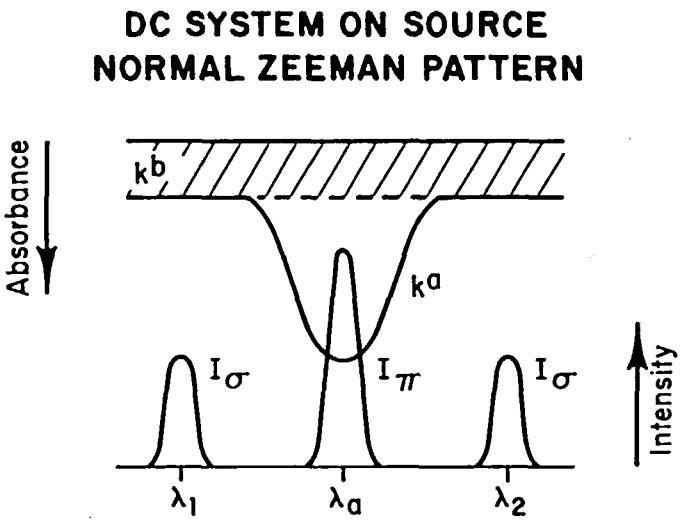

FIGURE 8. Background correction with a DC magnetic field on the source and an absorption line that displays a normal Zeeman pattern. (Adapted from de Loos-Vollebregt, M. T. C. and de Galan, L., *Prog. Anal. At. Spectrosc.*, 8, 47, 1985.)

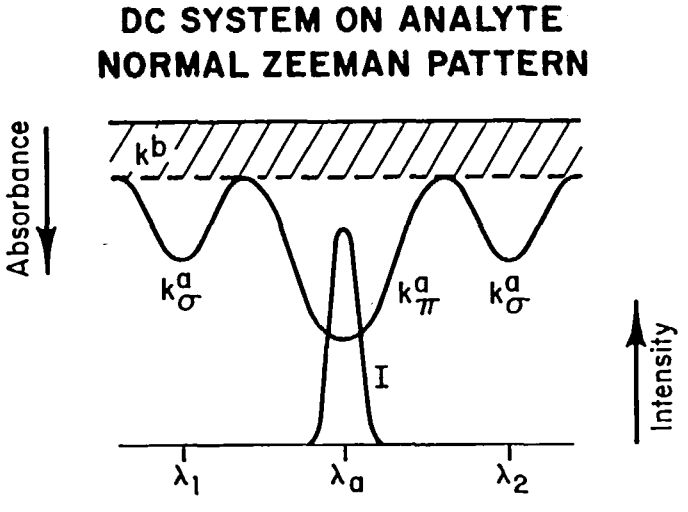

FIGURE 9. Background correction with a DC magnetic field on the analyte and an absorption line that displays a normal Zeeman pattern. (Adapted from de Loos-Vollebregt, M. T. C. and de Galan, L., *Prog. Anal. At. Spectrosc.*, 8, 47, 1985.)

I, of the source is reduced by the sum of $k^a + k^b$. In the sigma part of the cycle, the analyte absorbance is split into the two k^a absorbances which are beyond the profile of the source, so that the I signal measures only the k^b absorption. Again, the difference is the desired k^a_π.

When a DC magnet is used on the analyte, an important advantage over the situations where the magnet is on the source is that background correction occurs at precisely the same wavelength as used for measuring atomic absorption. In contrast, when the magnet is on the source, background is corrected at a neighboring wavelength.

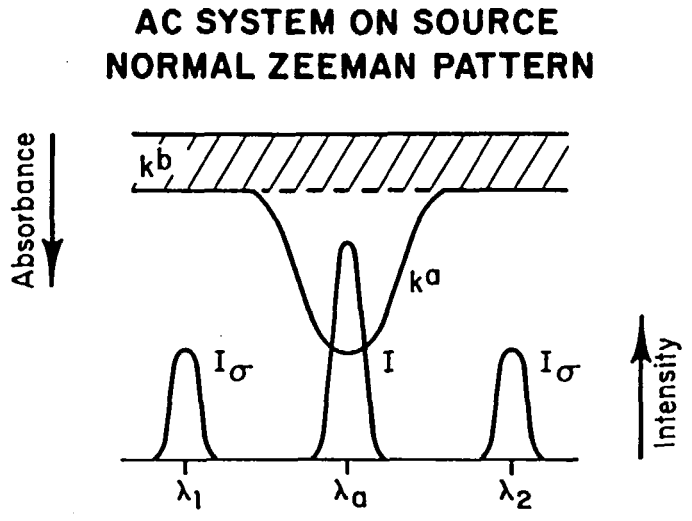

FIGURE 10. Background correction with an AC magnetic field on the source and an absorption line that displays a normal Zeeman pattern. (Adapted from de Loos-Vollebregt, M. T. C. and de Galan, L., *Prog. Anal. At. Spectrosc.*, 8, 47, 1985.)

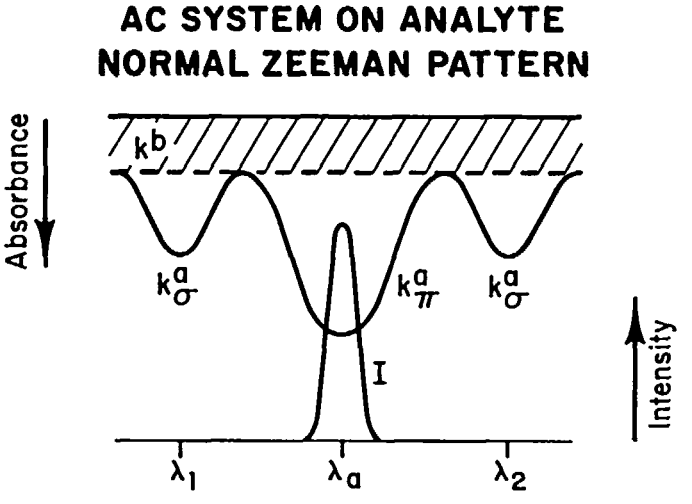

FIGURE 11. Background correction with an AC magnetic field on the analyte and an absorption line that displays a normal Zeeman pattern. (Adapted from de Loos-Vollebregt, M. T. C. and de Galan, L., *Prog. Anal. At. Spectrosc.*, 8, 47, 1985.)

An important advantage of the AC systems is that the polarizer is fixed in position. The two analytical signals are now the magnet-on and magnet-off signals. The AC system on the source is illustrated in Figure 10. When the magnet is off, the components collapse to the unsplit resonance line and the I signal measures the sum of background and atomic absorption. The fixed polarizer is set to reject the pi signal so, when the magnet is on, the radiation, I_σ, that bypassed the atomic peak (the sigma signal) measures background at a wavelength close to the absorption peak.

Similarly, when the AC system is used on the analyte (Figure 11), the magnet-off signal is the conventional AA plus background signal. The polarizer is set to reject the pi signal.

When the magnet is on, the analyte absorbance, k_σ^a, is shifted away from the source line and only background is measured. In contrast with the situation where the AC magnet is used on the source, the AC system on the analyte provides background correction at precisely the same wavelength as was used to measure AA. The AC system on the analyte is used on several commercial instruments.[36] In practice, the magnetic field strength need only be great enough to remove the displaced k_σ^a absorbance fully beyond the intensity profile, I, of the source. If the displacement is inadequate, the sigma signal will have some response for the analyte metal, thus reducing analyte sensitivity compared with ordinary AAS.

Thus, for lines that display a normal Zeeman pattern, the four alternatives of AC and DC magnet on the source or the analyte yield theoretically similar and convenient background correction. Problems arise, however, when these four alternatives are compared for transitions that display the anomalous Zeeman effect. Looking again at Figure 5 and comparing the pi and sigma components of normal and anomalous Zeeman patterns, the pi component is split into two components whose separation from the original line increases as the magnetic field strength increases. If the DC magnet system is used on the source or the analyte, and as the field strength is increased to split the sigma components, the pi-component split also increases, reducing AAS sensitivity. Therefore, if the field strength is increased to avoid loss of AAS sensitivity by failure to displace the sigma components, sensitivity will be lost by splitting the pi components.

Thus, for the DC magnet system, there is some optimum field strength for every anomalous wavelength that provides maximum sensitivity, and this sensitivity is usually significantly less than that of conventional AAS. The effect of magnetic field strength on the sensitivity for Ba and Ag relative to conventional AAS is shown in Figure 12. The figure illustrates the DC magnet on the analyte. When the field strength is 4 kG, the sensitivity for Ba is already within 10% of conventional AAS. Note however that for Ag at 328 nm, an anomalous transition, the peak sensitivity occurs at about 5 kG and is then only 60% of the conventional AAS signal. This situation applies similarly for the DC system on the source.

In the AC system, the pi component is rejected by the fixed polarizer and the signal is formed by the magnet-off and magnet-on signals. Thus the sensitivity loss by the splitting of the pi component is not a problem. The sigma wavelengths of all anomalous patterns are more separated from the unsplit line as a function of magnetic field than are those of normal patterns. Figure 13 compares AC and DC magnet systems for sensitivity loss for several anomalous transitions. The AC magnet was used on the analyte, but had it been used on the source the results would have been quite similar. Despite the anomalous splittings, the AC magnet system provided less than a 10% loss in sensitivity with magnetic fields of 6 kG or less, except for Se where 8 kG was necessary. Equally important, the DC magnet system required about 5 kG for As, 4 kG for Ag, 4 kG for Cr, and about 6 or 7 kG for Se. Any compromise field strength would have reduced the sensitivity even further.

The important fact to note is that for the AC magnet on the analyte the maximum field that is useful is that which separates the sigma peaks far enough to minimize overlap with the wings of the line in the source, about 6 to 9 kG for most important situations. The sensitivity loss of the AC and DC systems compared with conventional AAS is shown in Table 1 for several elements. A more extensive list is shown later.

Using an AC magnet of 8 kG field on the furnace, only 7 elements of the 40 most commonly determined suffer a sensitivity loss by Zeeman correction greater than 20%, and these are listed in Table 2. Some of these may result from the presence of several isotopes. The other elements suffer from hyperfine structure of the transition or some combination of this with isotope structure. However, note that no transition suffers a loss of sensitivity greater than half.

The instrumentation used for Zeeman background correction is a relatively simple modification of furnace instruments and their signal-handling systems. The signals for a typical

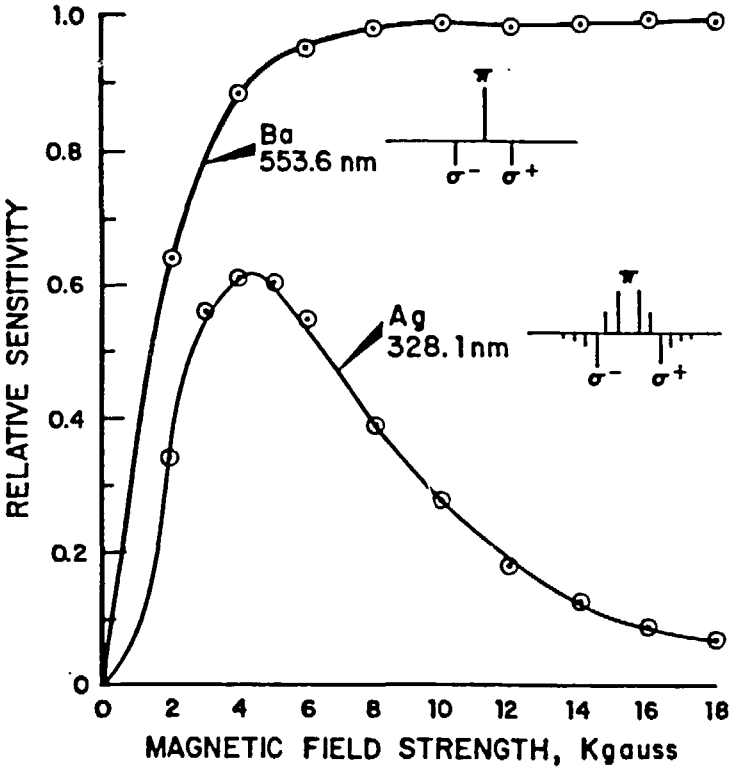

FIGURE 12. The relative sensitivity for Zeeman AAS compared to no background correction for two elements using a DC magnetic field on the analyte. The Ba line at 553.6 nm is typical of normal Zeeman patterns and the Ag line at 328.1 nm is representative of anomalous Zeeman patterns. (From Fernandez, F. J., Bohler, W., Beaty, M. M., and Barnett, W. B., *At. Spectrosc.*, 2, 73, 1981. With permission.)

system[42] are shown in Figure 14. In that portion of the AC power cycle when the magnetic field is off, an ordinary single beam absorbance signal, A_a, is generated which is proportional to the sum of the AA and the background. In the other portion of the cycle when the magnetic field is maximum, the polarized light from the source cannot be absorbed by the analyte atoms because the absorption wavelength has been displaced on either side of the source wavelength. Thus, the source radiation when the magnet is powered, also expressed as absorbance A_b, is attenuated only by the background. The Zeeman signal, ZAAS, is the difference between these two absorbance measurements:

$$ZAAS = A_a - A_b$$

Actually, of course, for those transitions where the displaced sigma peaks slightly overlap the source emission profile, the A_b signal will have some analyte dependence and there will thus be a small sensitivity loss compared with conventional AAS.

The source lamps are modulated at 120 Hz, while the current to the magnet is modulated at 60 Hz. In the typical practice, 60-Hz sine-wave modulation is used. During the portion of the cycle when the background A_b is measured, the field must be large enough to displace the sigma lines from the emission line. When the AC field is nearly zero during the AAS plus background A_a cycle, the magnetic field will be too small to split the sigma configurations. Thus, the sine-wave signal provides excellent results.

That the system works well is illustrated in Figure 15 where 1% NaCl produces a back-

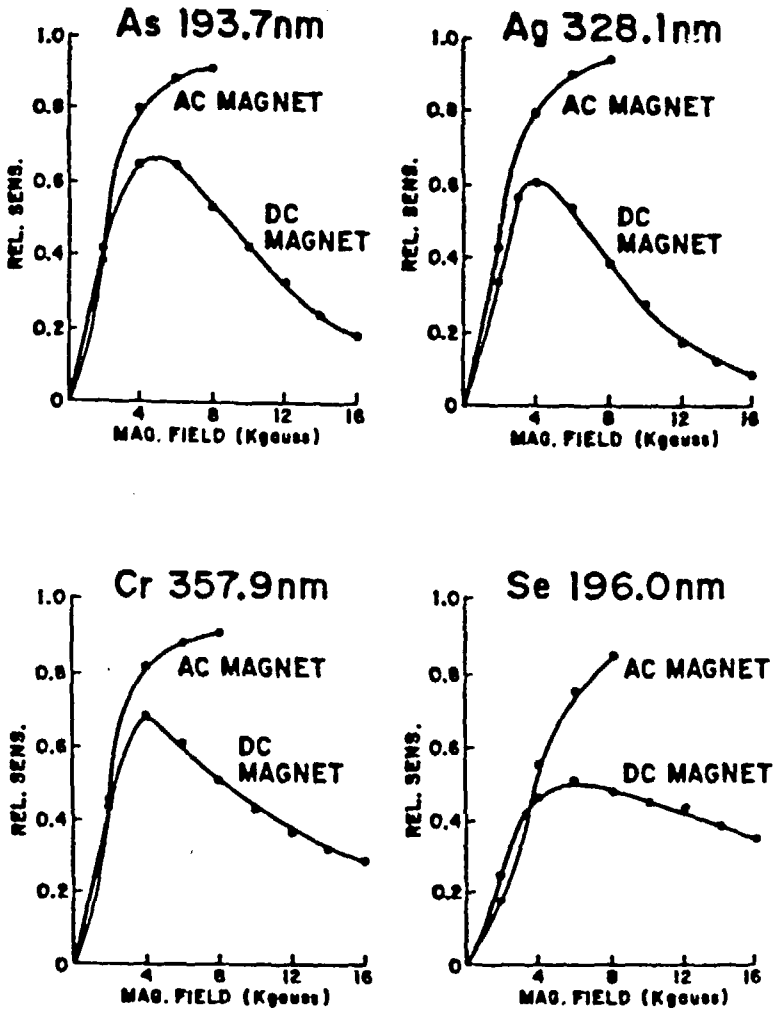

FIGURE 13. The sensitivity loss comparing AC and DC magnetic fields on the analyte. (From Fernandez, F. J., Bohler, W., Beaty, M. M., and Barnett, W. B., *At. Spectrosc.*, 2, 73, 1981. With permission.)

Table 1
RATIO OF ZEEMAN TO ORDINARY AAS

	DC system	AC system
Ag	0.3	0.9
As	0.4	0.9
Cr	0.4	0.9
K	0.3	0.6
Li	0.4	0.8
Mo	0.3	0.9
Na	0.3	0.9
Se	0.4	0.9

Note: Fixed field of 10 kG used for DC system and about 8 kG for the AC system.

Table 2
AC SYSTEM ON ANALYTE, RATIO OF ZEEMAN TO ORDINARY AAS

Element	(nm)	Zeeman class	Ratios
Be	234.9	N	0.5
Bi	223.1	A	0.6
Cu	324.8	A	0.5
Hg	253.7	N	0.6
K	766.5	A	0.6
P	213.6	A	0.7
Tl	276.8	A	0.7

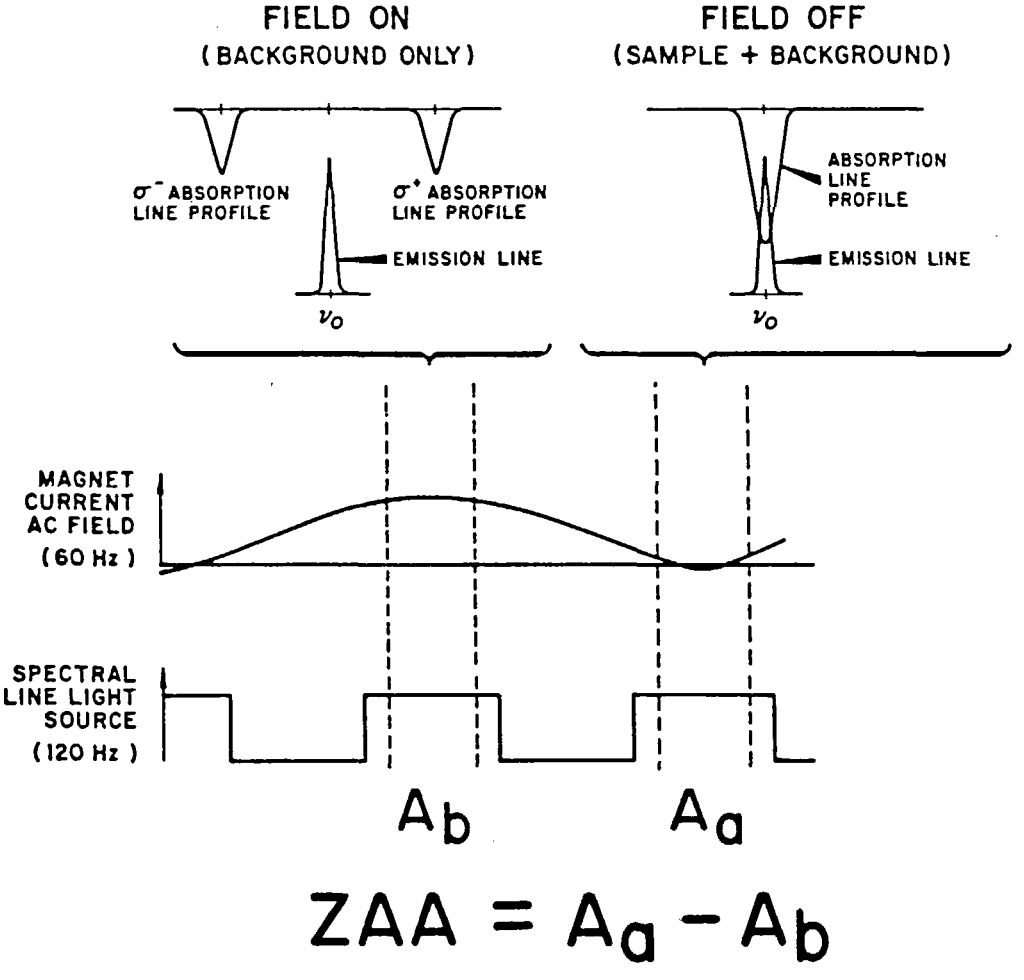

FIGURE 14. Signal handling for Zeeman AAS using an AC magnetic field on the analyte.

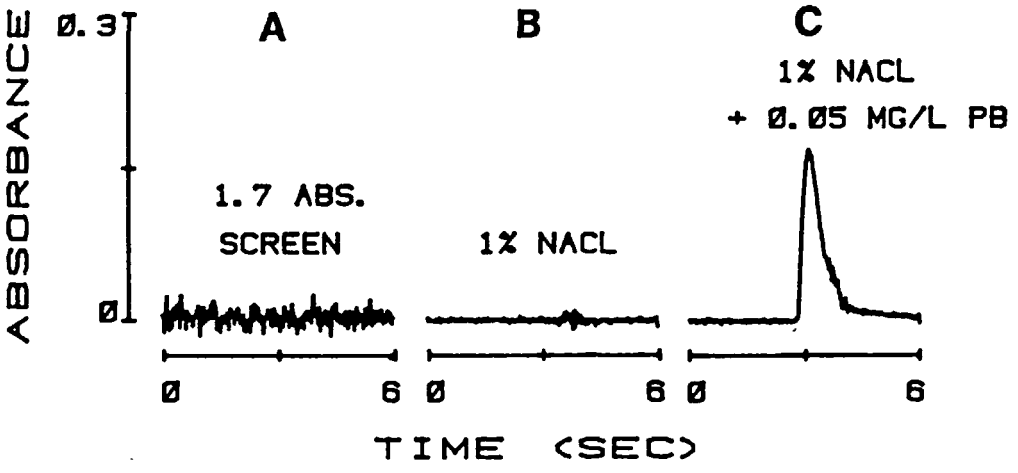

FIGURE 15. Noise increase resulting from energy loss due to background absorption. (From Fernandez, F. J., Bohler, W., Beaty, M. M., and Barnett, W. B., *At. Spectrosc.*, 2, 73, 1981. With permission.)

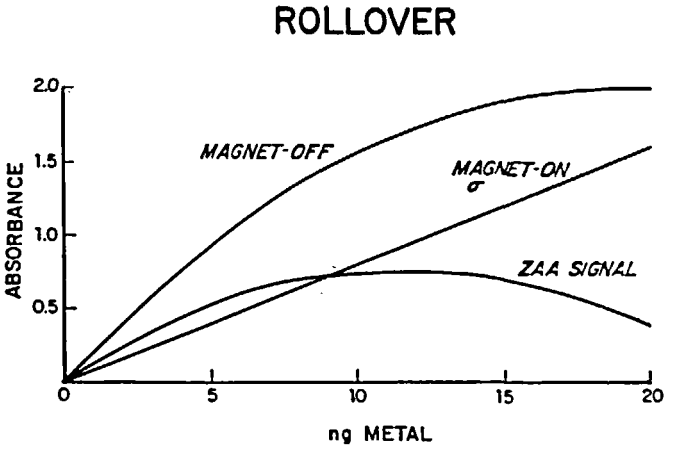

FIGURE 16. The cause of rollover using elemental conditions similar to those for Cu.

ground of 1.7 absorbance at the 283-nm line for Pb. While Zeeman AAS corrects for these large background signals, the light lost by the background will reduce the analytical signal-to-noise ratio. When the Pb-free NaCl was analyzed in panel B, there was no Pb signal, but the absorbance was noisy at the time when the background NaCl was generated. When a 1.7-A screen was put in the optical system (panel A), the noise under the background peak increased to the same amplitude recorded at the time the background had been generated.

When the Zeeman technique is used with a transition that does not fully separate the sigma absorbance from the wings, the corrected signal will have some dependence on the analyte. This is illustrated schematically in Figure 16. As we have shown previously, this will not be a serious problem for normal Zeeman transitions in either DC or AC magnet systems, or for anomalous transitions if the AC magnet system is used. The magnet-off signal, which is a conventional AAS signal, begins to bend at some high absorbance and will typically become asymptotic to the concentration axis at an absorbance which depends upon the stray light of the system. Since the sensitivity for the magnet-on signal, the sigma signal, is less than the magnet-off signal, it will remain more linear at a concentration where

the magnet-off signal has already become smaller in slope. In the example in the figure, the two curves have become equal in slope at about 12 ng of metal and the difference between the two curves, the Zeeman AA signal, has reached a peak. For higher concentrations, the magnet-on sigma absorbance signal is larger in slope than the magnet-off signal and the Zeeman AAS curve bends downward. This downward turn is called "rollover". It is troublesome because, if undetected, a large concentration can be erroneously reported as a very low value. Fortunately, in furnace AAS it is easy to detect and not very troublesome, particularly if integrated A signals are used.

While the situation in Figure 16 is schematic, it is roughly representative of Cu, one of the elements suffering the greatest loss of sensitivity, about 50%, using the AC magnet on the furnace. Those elements suffering less loss in sensitivity typically have a peak at higher absorbance and display less rollover. Using the AC magnet on the furnace, this loss of sensitivity is small for almost all the lines used for the elements frequently determined in the furnace, and thus the rollover problem is also small. The effect is frequently discussed in connection with the Zeeman technique because it remains an important problem when a DC magnet is used for anomalous transitions, especially for flame AAS.

In Table 3, we record some useful data for the lines of analytical importance in furnace AAS using a transverse AC magnetic field on the furnace. The columns for Zeeman class and Zeeman sensitivity ratio come from Fernandez et al.[41] The column of rollover absorbance comes from Reference 43. The calculated and experimental data for characteristic mass, a measure of analytical sensitivity, come from L'vov et al.[44] Their values use conditions intended to produce optimum characteristic mass data, and these values do not include the loss in sensitivity resulting from the use of Zeeman correction. Characteristic mass data for Zeeman AAS must be calculated by dividing these values by the Zeeman ratio data.

IV. SMITH-HIEFTJE CORRECTION

Background correction with a continuum source, proposed originally by Koirtyohann and Pickett,[3] has some disadvantages: (1) the alignment and superposition of the analyte and continuum sources are critical and are difficult to maintain; (2) some matrices provide interferences because they selectively absorb the background radiation; (3) the brightness of the continuum source limits the signal-to-noise ratio in many cases and thus the detection limits that are attainable. Smith and Hieftje[7] proposed that the source line be broadened and self-absorbed to provide some of the advantages of Zeeman correction, but at a lower cost.

The idea upon which the Smith-Hieftje (S-H) technique is based is illustrated in Figures 17 and 18. If a spectral light source, e.g., an HCL, is operated with usual conditions, the spectral profile that results is represented by the curve marked "low current". If the lamp is run at much higher current, more metal atoms are sputtered from the cathode into the space between the cathode and the lamp window. The absorption coefficient of these sputtered atoms is greatest at the line center, falling rapidly to smaller values away from the line center. Thus at high current, the emission is more intense, but more of the radiation at the center of the line is absorbed than in the wings. This has the effect of broadening the line and, if the current is large enough, producing a smaller signal at the center than in the wings, as shown in Figure 17. When the light from these two configurations is passed through the absorption cell, i.e., the flame or furnace, the resulting calibration curves of Figure 18 are generated. The low current curve is that usually observed in AAS. The high current curve produces a smaller absorption because the strongly absorbed center of the line has been depleted. Both curves will be similarly affected by background radiation, so the difference between the curves, the delta, will be a calibration curve of reduced sensitivity that has been corrected for the background absorption.

Correction by this means can be done without need for a second light source and this is

Table 3
ZEEMAN DATA

Element	Wavelength (nm)	Zeeman class[a]	Rollover (Å)	Characteristic		Ratio[c]
				Calculated	Experimental	
Ag	328.1	A	>2	1.1	1.2	0.91
Al	308.2	—	—	8.1	11.8	0.72
Al	309.3	A	0.8	—	10.0[d]	0.90
Al	396.2	—	>2	—	13.0[d]	0.90
As	193.7	A	1.3	—	17.0[d]	0.89
As	197.2	—	—	13.0	16.1	—
Au	242.8	A	1.6	6.4	7.3	0.84
B	249.7	A	0.5	—	700.0[d]	0.61
Ba	553.6	N	>2	0.63	7.3	0.96
Be	234.9	N	0.5	0.32	0.45	0.51
Bi	223.1	A	>2	—	15.0[d]	0.63
Bi	306.8	—	—	23.	22.0	—
Ca	422.7	N	>2	0.25	0.54	0.95
Cd	228.8	N	0.8	0.48	0.39	0.98
Co	240.7	A	—	6.6	5.4	0.85
Co	242.5	—	1.0	—	7.0[d]	—
Cr	357.9	A	1.6	1.6	1.8	0.88
Cs	852.1	—	>2	2.5	5.2	—
Cu	324.8	A	0.7	3.1	3.0	0.53
Er	400.8	—	—	2.7	23.0	—
Eu	459.4	—	—	2.2	9.7	—
Fe	248.3	A	0.8	2.7	2.8	0.92
Ga	287.4	—	1.3	9.1	9.8	—
Ge	287.4	N	>2		34.0[d]	0.90
Hg	253.7	N	0.3	54.	52.0	0.61
In	303.9	—	—	7.3	9.3	—
In	325.6	A	1.2	—	20.0[d]	0.91
Ir	264.0	—	1.0	—	250.0[d]	0.96
K	766.5	A	>2	0.66	0.9	0.61
Li	670.7	N	>2	0.46	1.1	0.85
Mg	285.2	A	1.0	0.32	0.30	0.91
Mn	279.5	A	1.1	1.6	1.7	0.91
Mo	313.3	A	>2	3.0	5.4	0.95
Na	589.0	—	>2	0.49	0.5	—
Na	589.6	A	>2	—	—	0.95
Ni	232.0	A	0.7	5.3	7.5	0.91
P	213.6	A	0.7	1320.	1240.0	0.70
Pb	283.3	N	1.5	13.	7.0	0.83
Pd	247.6	N	1.3	—	22.0[d]	0.91
Pt	265.9	—	1.1	—	95.0[d]	0.80
Rb	780.0	—	>2	1.7	2.5	
Rh	343.5	—	—	—	10.0[d]	
Ru	349.9	A	1.4	—	31.0[d]	0.90
Sb	217.6	A	1.4	—	38.0[d]	0.95
Sb	231.1	—	—	34.	30.0	—
Se	196.0	A	1.4	16.	19.0	0.88
Si	251.6	N	—	13.	67.0	0.98
Sm	429.7	—	>2	—	240.0[d]	
Sn	286.3	N	>2	13.	20.0	0.94
Sr	460.7	N	>2	0.3	0.95	0.98
Te	214.3	A	1.1	—	15.0[d]	0.93
Te	225.9	—	—	115.	116.0	—
Ti	364.3	—	>2	—	45.0[d]	—

Table 3 (continued)
ZEEMAN DATA

Element	Wavelength (nm)	Zeeman class[a]	Rollover (A)	Characteristic		Ratio[c]
				Calculated	Experimental	
Ti	365.3	A	—	10.	30.0	0.96
Tl	276.8	A	0.6	8.2	9.6	0.66
V	318.4	A	1.3	17.	19.0	0.77
Yb	308.8	—	—	—	2.5[d]	—
Yb	398.8	—	—	1.1	1.6	—
Zn	213.9	N	1.0	0.51	0.4	0.88

[a] Zeeman class: A = anomalous, N = normal.
[b] The characteristic mass data, both calculated and experimental, are from L'vov et al.[44] No background correction was used. Characteristic mass is defined as the mass of analyte in Pg that produces an integrated signal of 0.0044 A·s.
[c] The Zeeman sensitivity ratio is the Zeeman-corrected AAS characteristic mass divided by the characteristic mass using no correction. An AC magnetic field of 9 kG is assumed.
[d] Reference 43.

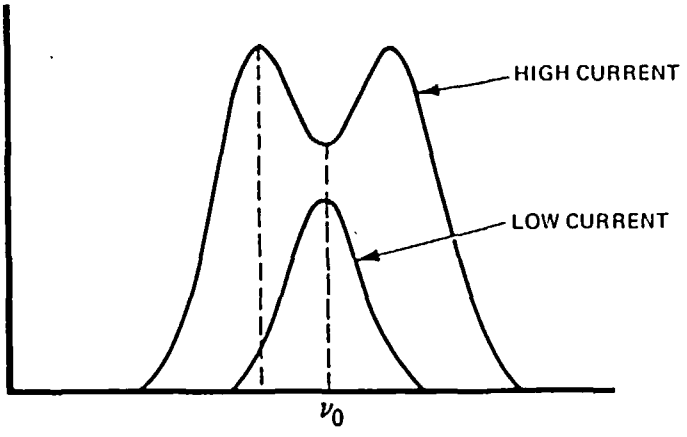

FIGURE 17. Schematic drawing of the emission line profile for a resonance line from a hollow cathode lamp at low and high current. (From Sotera, J. J. and Kahn, H. L., *Am. Lab.*, November 1982. With permission.)

an important advantage over continuum correction. Since the same source is used for the two measurements, the two beams follow the same optical path. In their paper, Smith and Hieftje argued that the correction was close to the analyte line, similar to the Zeeman technique, but that the rollover, or double-valued problem experienced by Zeeman correction, was absent. de Galan and de Loos-Vollebregt[46] showed that this was not true and that the smaller sensitivity to analyte shown in Figure 18 as the low current curve was analogous to the smaller sensitivity of the Zeeman correction curve. It is this smaller sensitivity in both cases that leads to the doubled-valued rollover condition.

How this happens can be explained from Figure 19, taken from a later paper of de Loos-Vollebregt and de Galan.[47] The A panel of Figure 19 represents the same situation shown in Figure 18, except that now the curves have been extended to higher concentrations. The low and high current curves become asymptotic to some absorbance which is proportional to the stray light in the system. For example, an asymptote at 2A would indicate that 1%

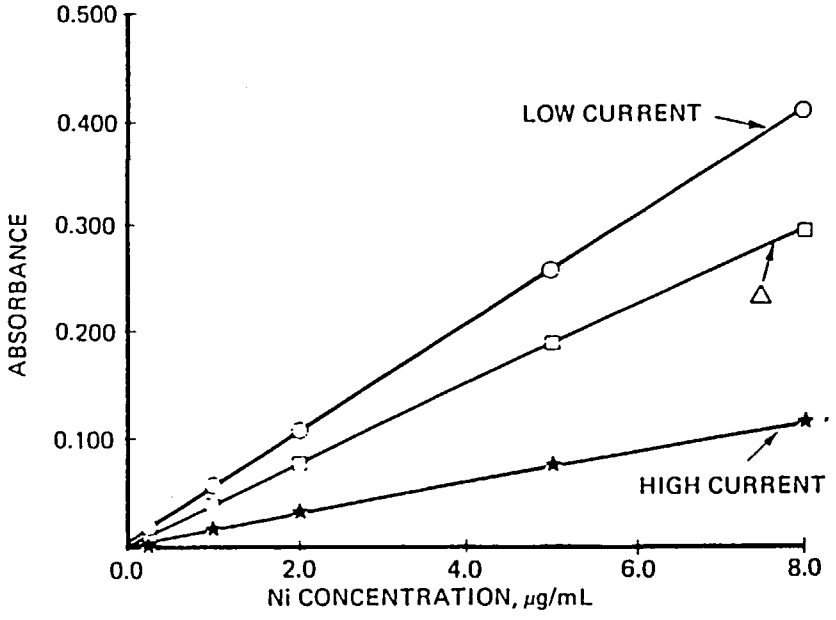

FIGURE 18. Ordinary and S-H analytical curves for Ni illustrating the reason for loss of sensitivity. (From Sotera, J. J. and Kahn, H. L., *Am. Lab.*, November 1982. With permission.)

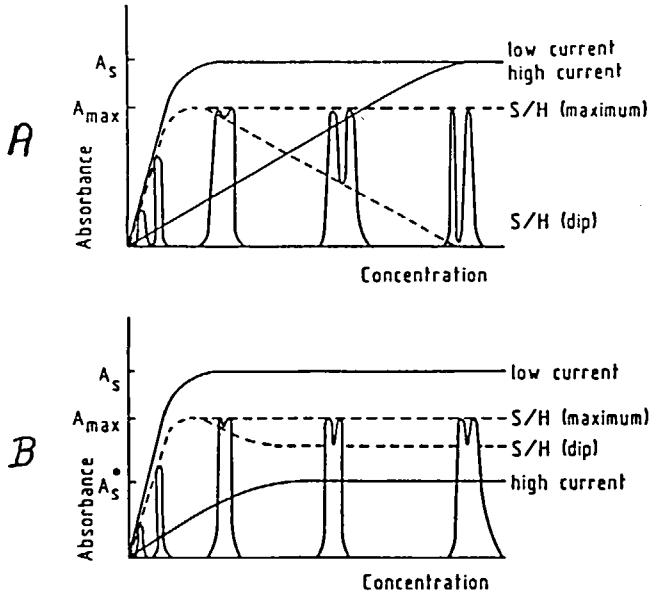

FIGURE 19. Calculated analytical curves for the S-H system for low current and high current. In (A), it is assumed that the limiting stray light causes both curves to be asymptotic to the same limiting absorbance. In (B), it is assumed that the stray light is larger during the high current pulse. The resulting S-H difference curves are plotted for both situations, including the dip levels. The curve is from de Loos-Vollebregt and de Galan.[47]

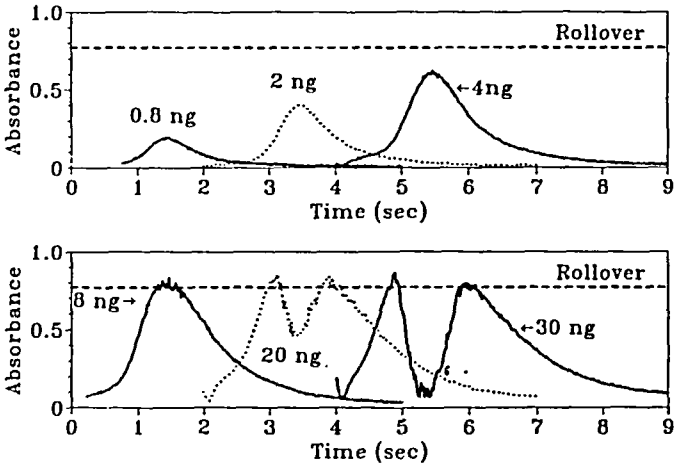

FIGURE 20. Absorbance profiles for Tl at various concentrations illustrating dip levels. (From Barnett, W. B., Bohler, W., Carnrick, G. R., and Slavin, W., *Spectrochim. Acta*, 40B, 1689, 1985. With permission.)

of the source radiation reaching the detector was unabsorbable by the analyte. The high current curve displays reduced sensitivity to the analyte and, after subtracting the two signals to produce the S-H analytical curve, accounts for the loss of sensitivity. At the concentration where the gross AA, low current curve and the high current curve have equal slopes, the corrected S-H curve will reach a peak. This is the same situation illustrated earlier for Zeeman AAS in Figure 16.

Within Figure 19 are shown absorption profiles, very much like those shown in Figure 17, at various concentrations of analyte. At higher concentrations of analyte in the flame or furnace, the absorption profile begins to develop the dip shown in Figure 19 for precisely the same reason that the same dip was found in Figure 17 in the HCL. The analyte absorption at the line center is greater than in the wings and eventually the dip appears. As the analyte concentration increases, the dip deepens and the difference curve approaches the concentration axis.

At this point, we must distinguish between the signals observed in flame AAS and those observed in furnace AAS. In the flame, the steady-state absorbance signal will be at the level of the dip. Thus, the flame S-H analytical curve and the flame Zeeman curve will display this troublesome double-valued rollover effect. In the furnace, however, the analyte gradually increases in the optical path and the absorbance rises until, at the rollover absorbance, it reaches a peak, and then at still increasing concentrations the signal diminishes. The effect is seen in real absorbance profiles for Tl in Figure 20. When all the analyte in the furnace has been vaporized, the concentration begins to diminish and the absorbance rises again to the previous maximum before falling back to zero.

In all of this, we assumed that the effect that caused the gross AA curve to become asymptotic to some absorbance A would have the same effect upon the BG signal. In A panel of Figure 19, both curves become asymptotic to the same absorbance. In the B panel, we assume that the stray light that caused the BG curve to reach some asymptote is different from that for the AA curve and that, in the BG situation, the stray light is greater. The analytical curve develops the same way as in the A panel for small concentrations of analyte, but when the BG curve reaches its lower asymptote, the dip can no longer increase. Therefore, the steady-state signal at the center of the dip will not continue indefinitely to smaller values as the analyte concentration rises. Correction with the D_2 source will not display this loss

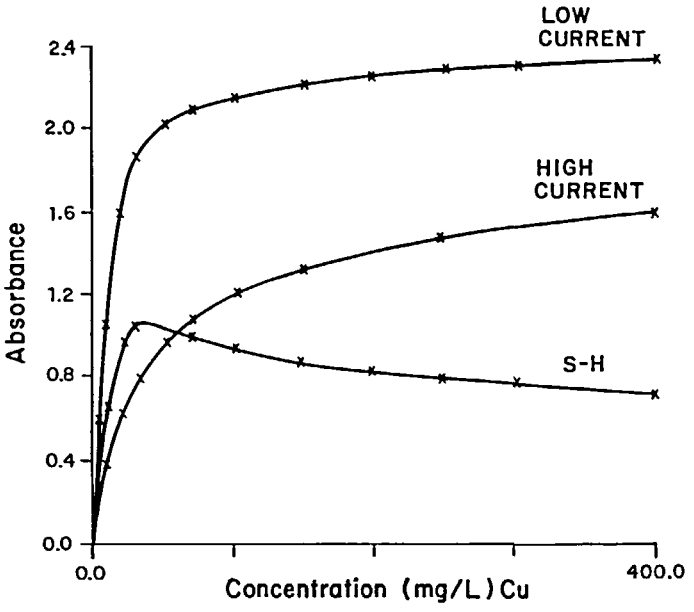

FIGURE 21. Experimental high and low current analytical curves for Cu in the flame. The low current and S-H curves are measured and the high current curve is calculated as the difference of the other curves. This also applies for Figures 22 to 24.

of sensitivity or the rollover effect because the correction signal is virtually independent of analyte absorption.

Since S-H-corrected curves displayed a large loss of sensitivity for many elements, de Galan and de Loos-Vollebregt[46] expected to find rollover (as in panel A of Figure 19) or significantly different stray light levels (panel B of Figure 19). The panel B situation was implied in the de Galan-de Loos-Vollebregt paper and they raised a question as to the source of the additional stray light and its influence on background correction. Curves for Cu, Fe, As, and Al were prepared by us, plotting the experimental gross AA and S-H curves using flame AA conditions for several metals. These are Figures 21 to 24. The high current, background curve (BG) was calculated by subtracting ordinates of the gross AA and the S-H curves.

Curves were prepared also for Ni, Mg, Cr, Pb, Zn, Cd, and V, but are not displayed here. While comparison of the S-H curves for elements like As and Al might imply that different mechanisms were active for different elements, careful examination of the full series of figures indicated that the situations were quite similar for the elements tested, differing only in degree. All of the curves differ from the D_2-corrected situation where the BG curve would coincide with the x axis, with essentially all of the BG radiation being stray light.

The sensitivity loss for the S-H system is found by comparing the slopes of the AA and S-H curves. Table 4 reports the flame AA sensitivity found from these experiments and includes the S-H sensitivity sacrifice calculated from these data. The term "remaining sensitivity" in Table 4 is 100% less the percent loss caused by the background corrector. The flame sensitivity in the table is micrograms per liter for 0.0044 absorbance. These data are compared with those taken from de Galan and de Loos-Vollebregt.[46] There is good qualitative agreement.

We believe that the low energy in the wings of the source radiation is the source of the unabsorbable stray light. It probably provides the energy that produces the stray light asymp-

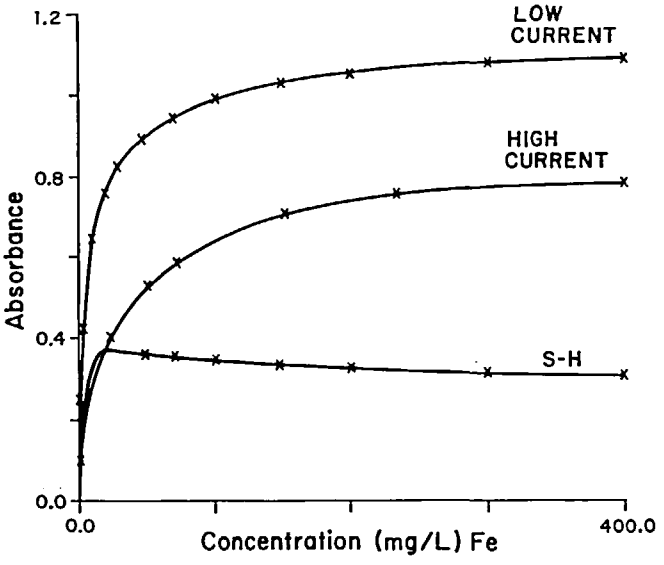

FIGURE 22. Experimental S-H analytical curves for Fe.

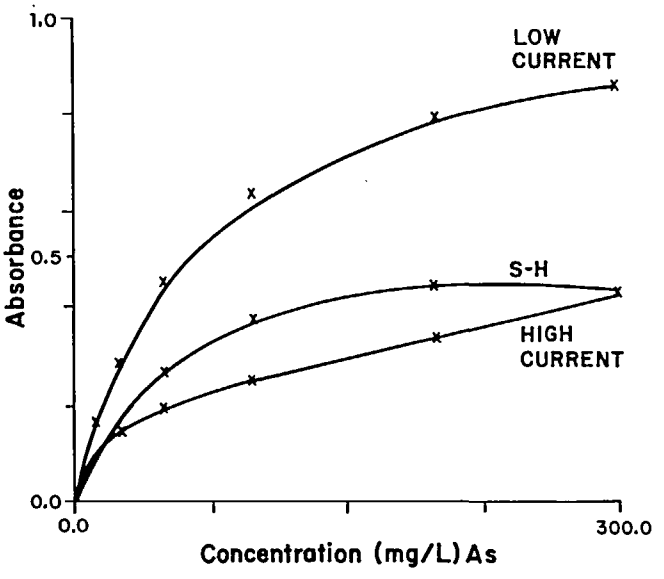

FIGURE 23. Experimental S-H analytical curves for As.

tote for most conventional AA calibration curves. In the high current mode, the amplitude of the energy in these wings increases greatly, producing the higher stray light level observed.

While this energy lies outside the bandwidth of the analyte absorption line, its intensity decreases rapidly with distance from the line center, and the energy is negligible at the extremes of even the narrowest slit width used in AAS.

V. SIMULTANEOUS CONTINUUM SIMAAC SYSTEM

The simultaneous multielement AA spectrometer (SIMAAC) system extensively developed by O'Haver and colleagues[15] adapts AA to a quite different set of instrumental param-

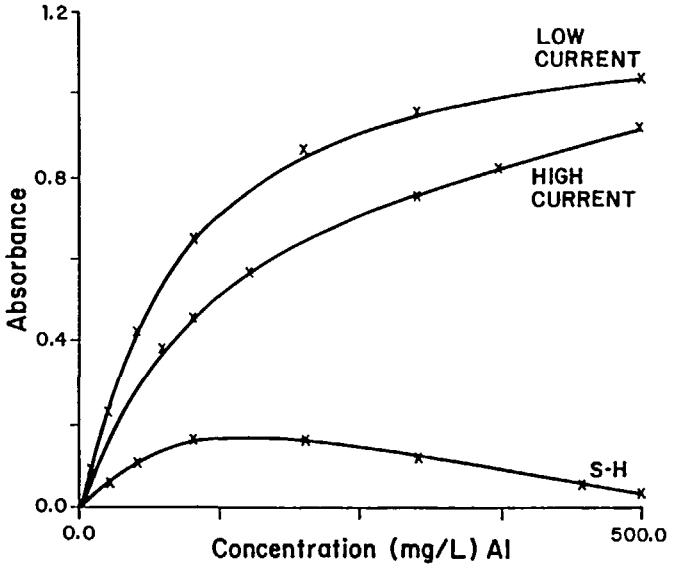

FIGURE 24. Experimental S-H analytical curves for Al.

Table 4
COMPARISON OF CALCULATED FLAME SENSITIVITY VALUES

	Observed value[a]		Remaining S/H sensitivity (%)	
Element	D_2	S/H	This work	Ref. 46
Aluminum	425	1750	25	25
Arsenic	430	625	69	—
Cadmium	17	19	89	90
Chromium	45	85	53	—
Copper	35	55	64	50
Iron	40	80	50	50
Lead (217 nm)	120	160	75	—
Lead (283 nm)	275	400	69	—
Magnesium	3	6	50	—
Nickel	55	80	69	—
Vanadium	650	4500	14	20
Zinc	8	11	73	—

[a] Sensitivity in micrograms per liter for 0.0044 A.

eters. The system diagram is shown in Figure 25. It uses a high-power continuum source, usually the 300-W Eimac xenon lamp, an echelle monochromator for high dispersion, and a bank of photomultipliers set at the wavelengths of analytical interest. Both a flame and furnace have been used to produce the sample vapor for the SIMAAC system. When a continuum is used for AAS, it is necessary to have high dispersion since the absorption linewidth in the flame or furnace is on the order of 0.01 nm or smaller. Walsh's original concept included the use of element sources to provide radiation of narrow spectral width without requiring a large, high dispersion monochromator. However, having given up this advantage of Walsh AAS, the SIMAAC system has the opportunity to correct background

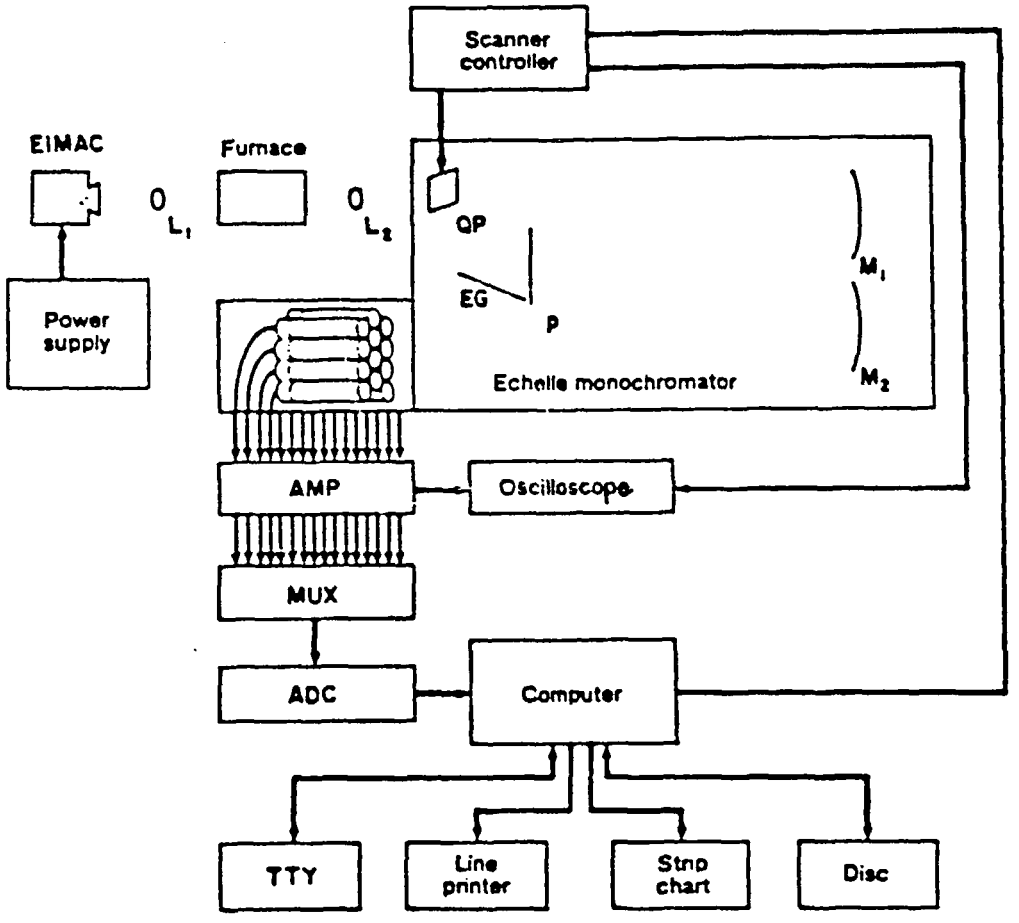

FIGURE 25. Block diagram of the SIMAAC system.

with the same source. A quartz plate is mounted within the monochromator (called scanner controller on the figure). When this plate is oscillated rapidly, the wavelength at the exit slits changes by a small amount, effectively scanning a short wavelength region adjacent to each line. Photometric measurements made when this plate is in different positions provide an absorption signal at various positions off the center of the line, as well as at the line center. These other absorptions can be used for background correction quite close to the analytical line.

The system has been used in other laboratories and, by now, several instruments have been assembled. Applications have been published and it is apparent that good analytical results are obtained with good background correction. The subject is not directly pertinent to this review, so further information should be sought elsewhere, e.g., the recent authoritative review by O'Haver and Messman.[48]

VI. CONTINUUM SOURCE BACKGROUND CORRECTION ERRORS

For the continuum source background corrector of Section II to work effectively, the average background absorption of the matrix materials over the spectral bandwidth of the monochromator must equal the background absorption at the center of the analytical line. Where this condition is not fulfilled, the background absorbs more or less of the continuum

radiation than it does the line source radiation, and an overcorrection or undercorrection error results. The most frequent of these spectral interferences results from atomic absorption of the background radiation by massive amounts of metals in the matrix, usually at secondary absorption lines for these elements. However, some of the structured absorption errors result from molecular absorption in the vapor phase.

Over the decades of flame AAS experience, very few reports of direct spectral line overlap have appeared, and these errors would appear even when background correction is not used. Koizumi[49] reviewed the earlier literature of direct spectral overlap and showed that several examples could be corrected using a Zeeman correction system. Slavin and Sattur[50] found that Pb interfered with Sb in the flame without background correction. This was hard to understand because the Pb line is at 216.999 nm and the Sb line is usually reported at 217.589 nm, the 0.59-nm separation being easily resolved with the monochromator. The interference of a Pb matrix on Sb is negligible if a 0.2-nm slit is used, but it is large if a 0.7-nm slit is used. The interference arises because there is a nonabsorbing line, 217.023 nm in the Sb lamp, which is only 0.024 nm from the Pb absorption line. Koizumi[49] showed that this overlap interference was removed using Zeeman correction and a slit width of 0.7 nm. Koizumi also showed a direct spectral overlap interference of Ni on Sb at the 231.147-nm Sb line. The Ni line is 0.05 nm away and the interference disappeared using Zeeman correction.

Probably the first identified example of the background overcorrection error was by Manning in 1978,[51] which showed that large amounts of Fe will produce such an error on the determination of Se at the 196-nm line. Vajda[52] listed a large number of potential interferences of this type and many have been demonstrated experimentally.

The paper by Vajda used flame AA where backgrounds are often very small. He indicated that some of the problems he identified were unlikely to be very serious in the flame. Since background is a much larger problem with the furnace and the amount of matrix is typically much larger relative to the analyte, these interferences are more severe in the furnace.

The listing by Vajda[52] and additional material from the literature have been reorganized in Table 5 for the important lines of most of the furnace analytes. He assumed that lines which display absorption and are separated by less than 1 nm will potentially interfere. Actually, stronger absorption lines or very large matrix amounts will introduce errors over a spectral gap larger than 1 nm, especially where a large slit is used, e.g., to improve the signal-to-noise ratio for determinations near the detection limit. Thus, there will be many more potential interferences than those shown here. We may have introduced a small rounding error in the $\Delta\lambda$ column which is insignificant for the purposes of this paper.

Many examples of these background correction errors have been published and they provide the powerful stimulus to use Zeeman correction for furnace AAS, where these problems are very few. The literature has frequently suggested that the method of additions be used to control errors when the furnace is used for analyses. However, the method of additions will not detect or correct background correction errors. The analyst must know from some other means which of his samples cannot be analyzed correctly if he is using continuum correction systems. Thus, the summary of reported problems in Table 5 will alert the cautious user to potential trouble.

An example of the effect of this background overcorrection error is shown in Figure 26, taken from the paper of Fernandez and Beaty.[59] The matrix consisted of solutions of Co, Fe, Cr, and Ni in the amount noted on the figure, with no Se present. The conditions for Se at 196 and 204 nm were used for analysis on a continuum-corrected instrument. When Zeeman correction was used for the same solutions, no overcorrection occurred.

Several problems of background overcorrection have been noted that have not yet been fully explained. Probably, they are like the effect of phosphate on Se and As,[55,60] where molecular P_2 is generated in the vapor phase of the furnace and the molecular bands absorb

Table 5
POTENTIAL OVERCORRECTION ERRORS

Analyte λ	Matrix (λ)		Δλ	Ref.
193.7 As	Ag	193.2	0.5	—
	Phosphate		—	55
	Al			56—58
196.0 Se	Bi	196.0	0.1	—
	Fe	195.4	0.6	51, 53, 59
	Phosphate		—	55, 60
	Co	197.4	1.4	59
204.0 Se	Cr	203.9	0.1	59
	Ni			59
208.9 B	Ir	208.9	0.01	—
208.9 Ir	B	208.9	0.01	—
		209.0		—
213.6 P	Fe	213.6	—	61
213.9 Zn	Te	214.3	0.4	52
	Fe	213.6	0.3	62
214.3 Te	Zn	213.9	0.4	52
	Sn	214.9	0.6	
	Phosphate		—	53, 54
216.5 Cu	Fe	216.7	0.2	
	Pb	217.0	0.5	
	Pt	216.5	0.01	
217.0 Pb	Cu	216.5	0.5	52
	Sb	217.6	0.6	49, 52
	Ni	216.6	0.4	—
	Fe	216.7	0.3	—
217.6 Sb	Pb	217.0	0.6	49, 50
	Cu	217.9	0.3	52
	Co	217.5	0.1	53
	Fe	217.8	0.2	53
217.9 Cu	Fe	217.8	0.07	
	Pb	217.0	0.9	
	Sb	217.6	0.3	
223.1 Bi	Cu	223.0	0.1	52, 53
224.6 Sn	Cu	224.4	0.2	
	Pb	224.7	0.1	
227.7 Bi	Re	227.5	0.2	
	Sn	226.9	0.8	
228.8 Cd	As	228.9	0.1	
	Phosphate			55, 63, 64
231.1 Sb	Ni	231.1		
232.0 Ni	Sn	231.7	0.3	
234.9 Be	As	235.0	0.1	
235.5 Sn	As	235.0	0.5	
240.7 Co	Ru	240.3	0.4	
242.5 Co	Au	242.8	0.3	
	Sn	242.9	0.5	
242.8 Au	Co	242.5	0.3	53
244.8 Pd	Cu	244.2	0.6	
	Ru	245.5	0.7	
247.6 Pd	Fe	248.0	0.3	
248.3 Fe	Cu	249.2	0.9	
	Pt	248.7	0.4	
248.8 Er	Cu	249.2	0.4	
	Pt	248.7	0.1	
	Fe	248.3	0.5	

Table 5 (continued)
POTENTIAL OVERCORRECTION ERRORS

Analyte λ	Matrix (λ)		Δλ	Ref.
250.7 Si	Fe	250.1	0.6	
251.4 Si	Fe	251.1	0.3	
251.6 Si	Fe	252.3	0.7	
	Co	252.1	0.5	
	V	252.0	0.4	
252.1 Co	Fe	252.3	0.1	
	V	252.0	0.2	
252.4 Si	Co	252.1	0.3	
	Fe	252.3	0.1	
253.6 Hg	Fe	253.6		65
	Co	253.6		
265.9 Pt	Ir	266.5	0.6	
	Sn	266.1	0.2	
271.9 Fe	Ga	272.0	0.07	
	Ta	271.5	0.4	
271.9 Pt	Fe	271.9		65, 66
276.8 Tl	Pd	276.3	0.5	
279.5 Mn	Mg	279.5		
	Pb	280.2	0.7	
279.8 Mn	Pb	280.2	0.4	
280.1 Mn	Pb	280.2	0.1	
283.3 Pb	Pt	283.0	0.3	
	Sn	284.0	0.7	
	Os	283.9	0.6	
285.0 Ir	Mg	285.2	0.2	52
287.4 Ga	Pb	287.3	0.1	
	Fe	287.4		62
294.4 Ga	Fe	294.8	0.4	
	V	294.1	0.3	
299.8 Pt	Fe	299.4	0.4	
	Ni	300.2	0.4	
	Pd	300.3	0.5	
303.9 In	Fe	303.7	0.2	
	Ni	303.8	0.1	
	Sn	303.4	0.5	
306.6 V	Bi	306.8	0.13	
	Pt	306.5	0.2	
306.8 Sb	Bi	306.2	0.7	
313.3 Mo	Ni	313.4	0.1	
	Ir	314.0	0.7	
324.8 Cu	Ni	324.3	0.4	
	Pd	324.3	0.4	
327.4 Sc	Ag	328.1	0.7	
	Cu	327.4	0.04	
	Rh	328.1	0.7	
327.4 Cu	Ag	328.1	0.7	
	Rh	328.1	0.7	
328.1 Ag	Cu	327.4	0.7	
	Rh	328.1	0.1	
	Yb	328.9	0.8	
	Zn	328.2	0.1	
338.3 Ag	Ni	338.1	0.2	
341.5 Ni	Co	341.3	0.2	
	Pd	342.1	0.6	

Table 5 (continued)
POTENTIAL OVERCORRECTION ERRORS

Analyte λ	Matrix (λ)		Δλ	Ref.
343.5 Rh	Ni	343.3	0.2	
	Ru	343.7	0.2	
345.2 Re	Co	345.4	0.2	
346.0 Re	Co	345.5	0.5	
346.5 Re	Co	346.6	0.1	
349.9 Ru	Co	350.2	0.3	
	Ba	350.1	0.2	
	Ni	349.3	0.6	
352.4 Ni	Co	352.7	0.2	
356.8 Lu	Ni	356.6	0.14	
	Ru	357.0	0.2	
357.9 Cr	Fe	358.1	0.2	
	Nb	358.0	0.1	
359.3 Cr	Ni	359.8	0.5	
360.5 Cr	Ni	361.0	0.5	
364.3 Ti	Pb	364.0	0.3	
368.4 Gd	V	368.8	0.4	
	Pb	368.3	0.1	
371.8 Tm	Fe	372.0	0.2	
391.2 Sc	Eu	390.7	0.5	
398.8 Yb	Ti	399.0	0.2	
405.8 Gd	Nb	405.9	0.07	
	Pb	405.8	0.04	
410.2 Y	Ho	410.4	0.2	
	In	410.2	0.1	
	Tm	410.6	0.4	
410.4 Ho	In	410.2	0.2	
	Tm	410.6	0.2	
	Y	410.2	0.2	
419.5 Dy	Tm	418.8	0.7	
421.2 Dy	Rb	421.5	0.3	

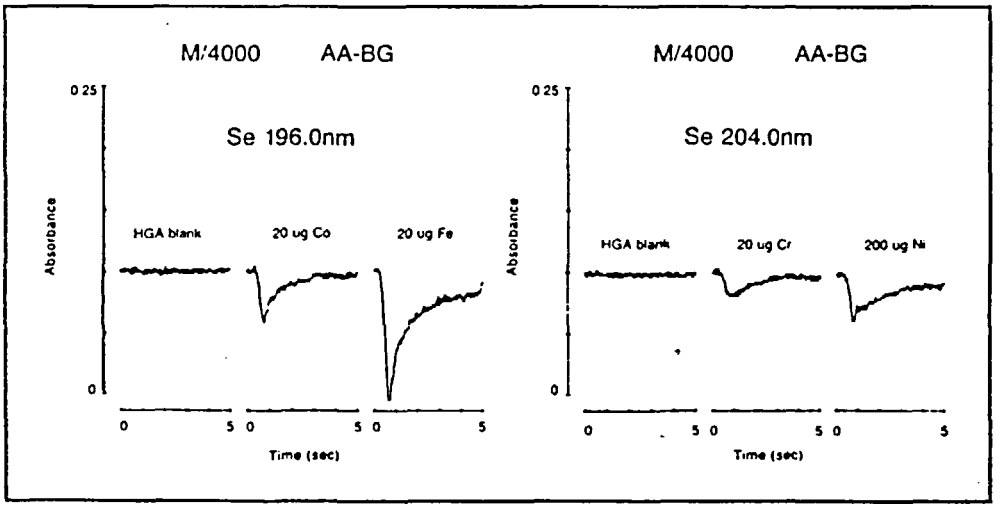

FIGURE 26. Continuum source overcorrection errors for Se at 196 and at 204 nm resulting from large amounts of Co, Fe, Cr, and Ni. (From Fernandez, F. J. and Beaty, M. M., *Spectrochim. Acta*, 39B, 519, 1984. With permission.)

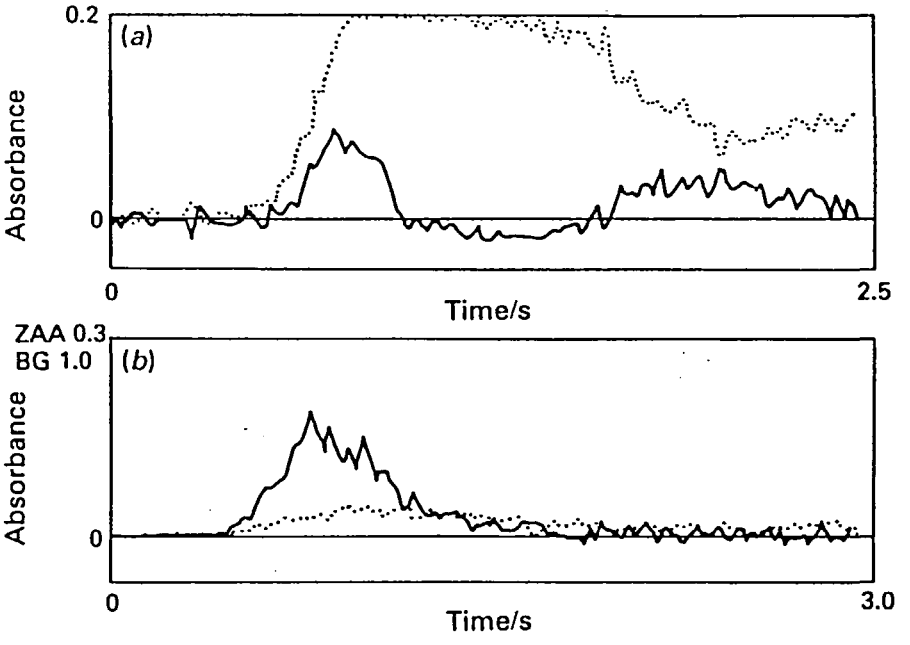

FIGURE 27. The signal and background for As in fish tissue comparing continuum source correction in (a) and Zeeman correction in (b). In both cases, the signal is the solid line and the background is the dotted line. (From Welz, B. and Schlemmer, G., *J. Anal. At. Spectrom.*, 1, 119, 1986. With permission.)

the continuum radiation. An example in fish tissue is shown in Figure 27. Cadmium in many matrices, especially in the presence of phosphate, exhibits overcorrection with a continuum corrector. This was shown (but not explained) in Slavin and Manning,[63] Völlkopf et al.,[64] and Welz and Schlemmer,[55] and there were no problems when Zeeman correction was used.

Pruszkowska and Barrett[56] confirmed an earlier finding by Riley[57] that Al interfered with As at 193.696 nm with a continuum corrector, but the effect was not a problem with Zeeman correction. An illustration from their paper is shown in Figure 28. Riley[58] recently speculated that the interference arises from the doubly ionized Al line at 193.58 nm and the singly ionized Al lines at 193.45 and 193.47 nm. This is not an overcorrection problem since the As signals are larger in the presence of Al, but we do not yet understand the spectroscopy of this situation.

Most of this material on errors with continuum source correction deals with systematic problems resulting from the spectral nature of the correction radiation and of the absorption or scatter of the matrix. Thus, the errors are called spectral correction errors. The larger problem with continuum source correction with a separate source relates to the difficulties associated with adjusting the two sources so that their beams traverse the same region of the furnace and do not change differently with respect to time during the measurement. It is very difficult to keep these relationships controlled during the lifetime of the instrumentation.

In a situation that is probably similar to many others, Dabeka[67] sent samples of infant formulas and milk to nine different, presumably experienced, laboratories for furnace determination of Pb. Only one of those laboratories got satisfactory results. A careful check of the laboratories convinced Dabeka that the errors were mostly a result of inadequate background correction, although the analytical background was only about 0.2 in these situations. In an interesting response to that paper, Andersen[68] showed that the samples

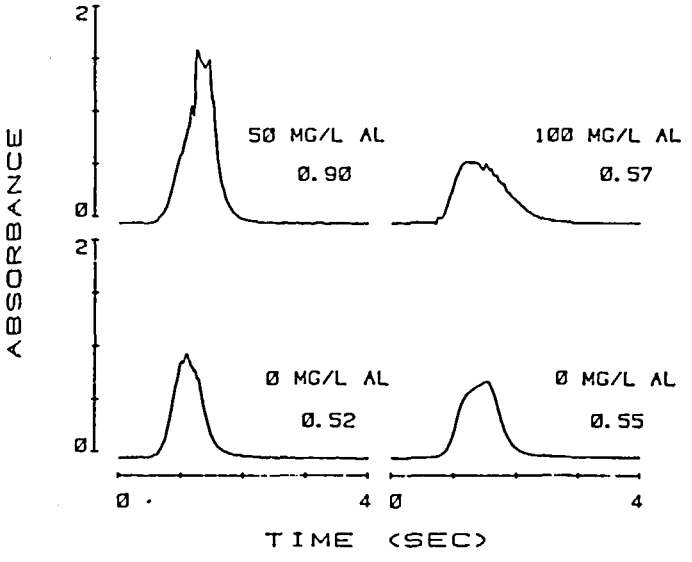

FIGURE 28. The interference of Al on 2 ng of As at 193.7 nm comparing continuum source correction (left-hand panels) and Zeeman correction (right-hand panels). With no Al present (lower panels), both systems provided similar integrated absorbance signals. In the presence of Al, continuum source-corrected results were almost a factor of two in error, while even larger amounts of Al had no effect on As using Zeeman correction. (From Pruszkowska, E. and Barrett, P., *Spectrochim. Acta*, 39, 485, 1984. With permission.)

studied by Dabeka were easily analyzed for Pb using Zeeman background correction and stabilized temperature platform furnace (STPF) conditions.

Other workers have shown that the energy distribution is not uniform across any of the sources used in AAS[69] and that the atomic vapor distribution is not uniform over the cross section of the furnace tube.[70] Thus, even if the two light sources could be adjusted so that their axes coincided, they would be sampling the atomic vapor in a different way. Thus, even well-adjusted continuum-corrected instruments are prone to quantitative errors. When instruments and light sources have been used for a considerable time in the laboratory, these problems increase and become insidious. They are difficult to diagnose and difficult to fix. These alignment problems provide the principal incentive for using Zeeman and S-H correction systems.

VII. ZEEMAN BACKGROUND CORRECTION ERRORS

With Zeeman background correction, problems associated with the spatial alignment of source and background beams are eliminated since a single source is used to measure both analyte and background absorption. If the magnet used to produce the Zeeman effect is placed around the analyte atoms, correction is made at the exact analyte wavelength. When used with the STPF technique,[71] complex samples may be analyzed, often with detection limits equal to those obtained in simple aqueous solutions using continuum correction. While very few Zeeman interferences have been found, several have been reported.[62,65,66,72-74] In 1978, Stephens and Murphy[65] demonstrated the first examples of spectral interference errors associated with Zeeman background correction. They used a variable DC magnet on the line source, thus background correction was made slightly off the analyte wavelength. Using a flame atomizer, they showed correction errors that varied in direction and magnitude with

field strength. There appear to be some typographical errors in reporting wavelengths in that paper, but evidently they found errors from 2000 and 3000 mg/ℓ Co (253.649 nm) in the determination of Hg at the primary resonance line of 253.652 nm, and from as little as 100 mg/ℓ Pt (271.904 nm) in the determination of Fe at the alternate 271.902-nm line.

Massmann[75] observed an increase in the measured background at the Bi 306.772-nm line using a variable DC magnet around an air-acetylene flame. The difference between the "real" and "measured" background absorbance increased with field strength and was attributed to the Zeeman splitting of OH rotational bands that were nearly coincident with the Bi absorption line. Such an interference would probably not exist in the graphite furnace due to the desolvation that occurs during the drying and thermal pretreatment steps.

Wibetoe and Langmyhr[62] used an AC magnet positioned transverse to the graphite tube and found overcorrection for Fe in the determination of Ga at 287.424 nm and Zn at 213.856 nm. Iron has absorption lines at 287.417 nm (0.007 nm from the Ga line) and at 213.859 nm (0.003 nm from the Zn line). In the Ga determination, as little as 5 μℓ of 20 mg/ℓ caused an overcorrection. Due to the differences in volatilities of Zn and Fe, it was considered likely that the careful selection of furnace parameters would provide time-separated signals that would be free of this problem.

Recently, Wibetoe and Langmyhr[72] examined the effect of Co, Mn, and Ni on the determination of 30 elements at 53 different wavelengths using Zeeman background correction. With an atomization temperature of 2100°C and Zeeman background correction, 0.1% Co produced an overcorrection at the alternate 267.7-nm Au line. Like Stephens and Murphy,[65] they also found a correction problem from Co on the determination of Hg at the primary 253.60-nm resonance line. The magnitude and the direction of the correction error varied with the Co concentration. However, the largest error was produced when deuterium background correction was used. A small overcorrection error was observed from Co at the 249.7-nm B line. No further studies were conducted since the interference was small and B is seldom determined in the furnace.

In most of the commercial Zeeman instruments, background correction is achieved by using an AC magnet transverse to the optical axis. If matrix absorption lines or bands (background) that are very close to the analyte wavelength exhibit Zeeman splitting, correction errors may occur. Figure 29 illustrates two such hypothetical cases.

In panel A, both a matrix and analyte absorption line are within the spectral bandpass of the monochromator. During the magnet-off cycle, the analyte absorption line (solid line) is centered over the source emission line (I), while the matrix line (dashed line) is displaced such that there is no overlap with source emission. Thus the source intensity is reduced only by analyte absorption. During the magnet-on (background) cycle, Zeeman splitting occurs and a sigma component (shown as σ_M^+) is displaced so that it overlaps the source emission line. Thus there is absorption from the matrix that is not present during the magnet-off cycle. The result is an overcorrection of the analytical signal.

Panel B shows an example where the matrix absorption line (dashed) overlaps the emission line (I) from the source. This causes some absorption that is not related to the analyte concentration. If no Zeeman splitting occurs, the contribution by the matrix to the absorption signal is equal in both the magnet-on and the magnet-off cycles. However, if Zeeman splitting occurs (as in panel B) such that the sigma component is shifted away from the source emission line, the measured background will be reduced and the analytical signal will be undercorrected.

Figure 30 shows the results obtained when atomizing 5 μg of Co at the Hg 253.6-nm wavelength using a Hg EDL and a spectral bandpass of 0.7 nm. Using 2000°C and wall atomization (panel A), there is considerable overcorrection of the analytical signal. For clarity, both the background profile and the Zeeman-corrected profile have been displaced above the baseline. This indicated that the Hg line from the source did not overlap the Co

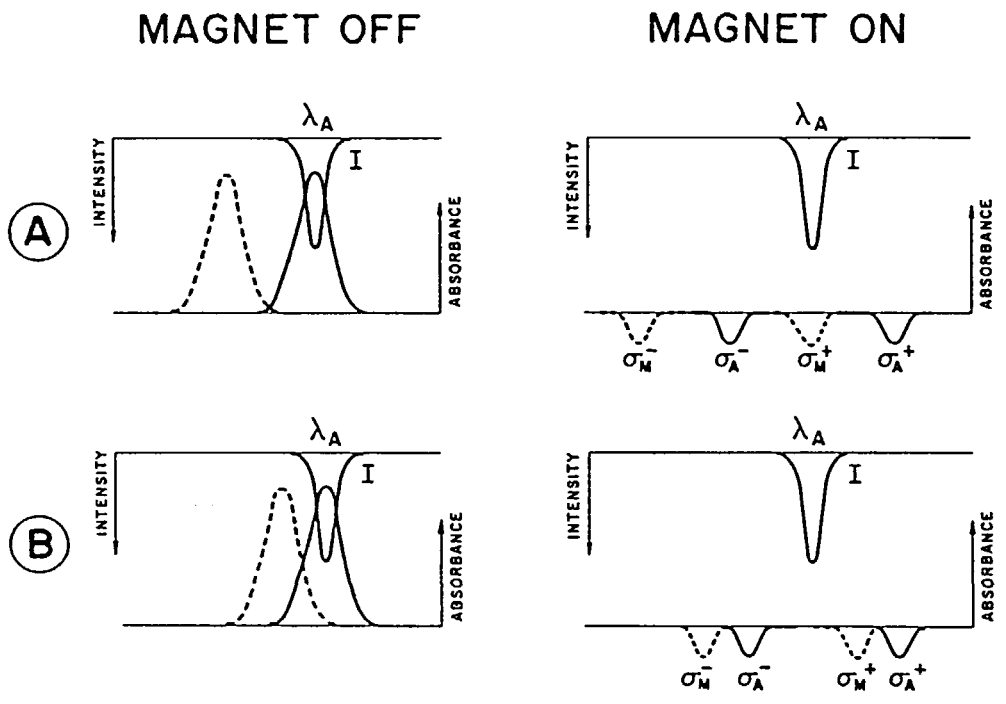

FIGURE 29. Schematic diagrams of the situations producing interferences in Zeeman-corrected AAS systems. The upper A panels will produce overcorrection and the lower B panels will produce undercorrection. (From Carnrick, G. R., Barnett, W., and Slavin, W., *Spectrochim. Acta*, 41B, 991, 1986. With permission.)

absorption with the magnet off, but during the magnet-on cycle, a sigma component from the Co absorption line was shifted on top of the Hg absorption line. This is the panel A situation from Figure 29. Using STPF conditions for the determination of Hg from the platform, a Pd matrix modifier, but atomizing at 2000°C (Figure 30, panel B), showed that the background absorbance was reduced fivefold, but there was still some overcorrection. However, when the atomization temperature was reduced to 1000°C as recommended for STPF conditions, this was below the appearance temperature of Co, and panel C showed that there was no background absorbance and no overcorrection. As a result, the determination of Hg in the presence of high concentrations of Co should pose no practical problem if modern platform techniques are used.

Standard furnace conditions[43] were used for the determination of Fe at the alternate 271.9-nm line. The Pt standard was prepared from ultrapure ammonium hexachloroplatinate (Spex Industries, Metuchen, N.J.). In the determination of Fe in the presence of Pt at the alternate 271.9-nm line, the Pt absorption lines overlap slightly the Fe emission line as in Figure 29, panel B. As a result, splitting of the Pt absorption line causes a reduction in the background measured during the magnet-on cycle. The result is a net positive signal in the absence of any deliberately added Fe analyte. This is shown in Figure 31. To verify that the signal obtained from the Pt was not from Fe contamination of the Pt, both the Fe standard and the Pt standard were run at the primary 248.3-nm Fe line. The Fe standard showed the expected fourfold increase in integrated absorbance at this more sensitive line. If all of the signal observed from the Pt standard in Figure 31 was from Fe contamination, it should also show a fourfold increase in integrated absorbance when run at the 248.3-nm line. However, instead of increasing, the integrated absorbance decreased about 40%. This indicated that while there was a small Fe contamination in the Pt standard the majority of the signal at the 271.9-nm line was an overlap problem. Due to the similar volatility of Fe and Pt, it is unlikely

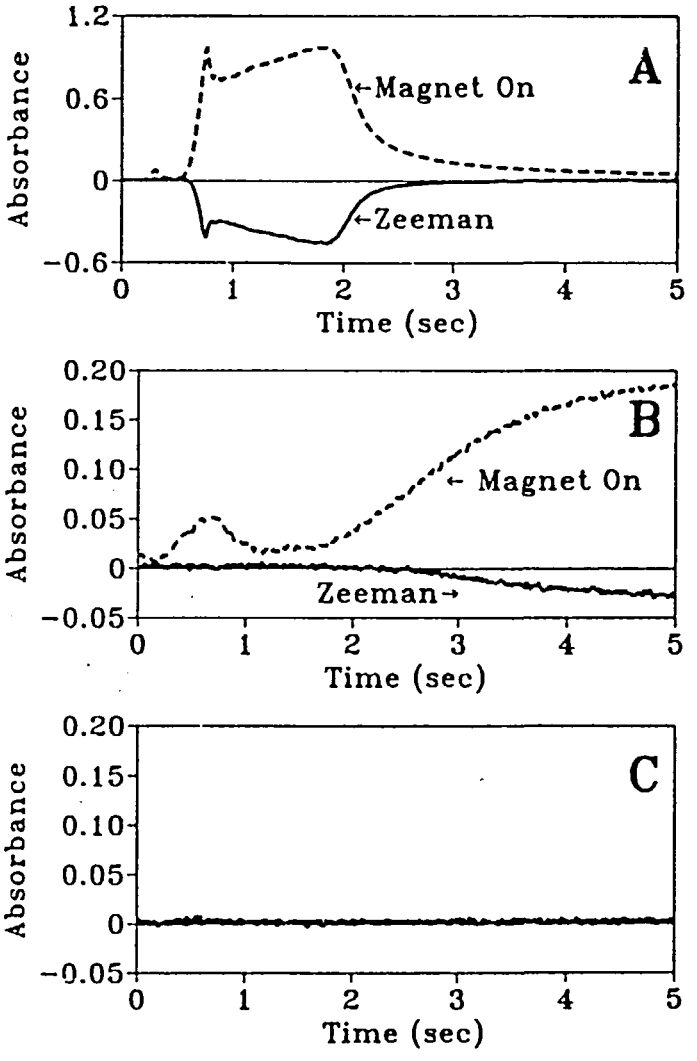

FIGURE 30. The Zeeman overcorrection error produced by Co at the Hg line at 253.6 nm. In (A), the Zeeman and background (magnet on) signals are recorded for 5 μg of Co. In (B), the same amount of Co has been atomized from the L'vov platform in the presence of Pd as a matrix modifier. In (C), the same conditions were used, but the atomization temperature was reduced to 1000 from 2000°C used in (A) and (B). (From Carnrick, G. R., Barnett, W., and Slavin, W., *Spectrochim. Acta*, 41B, 991, 1986. With permission.)

that this problem could be eliminated as the result of careful selection of furnace parameters. Equal amounts of Pt and Fe result in a correction error of about 2.5%.

Recently, Cd was determined in a solid flexible PVC material using the Cd line of low sensitivity at 326.1 nm.[76] In both the PVC material and the aqueous standard (which contained a matrix modifier of ammonium phosphate and magnesium nitrate), the Zeeman-corrected signal was displaced below the baseline following the peak. The Zeeman background-corrected signal and the single-beam signal (in this case background) from ammonium phosphate are shown in Figure 32. The ZAA profile shows an overcorrection which corresponds to a peak in the single-beam profile. The overcorrection was also obtained using H_3PO_4 instead of ammonium phosphate. Since both the ammonium phosphate and the H_3PO_4

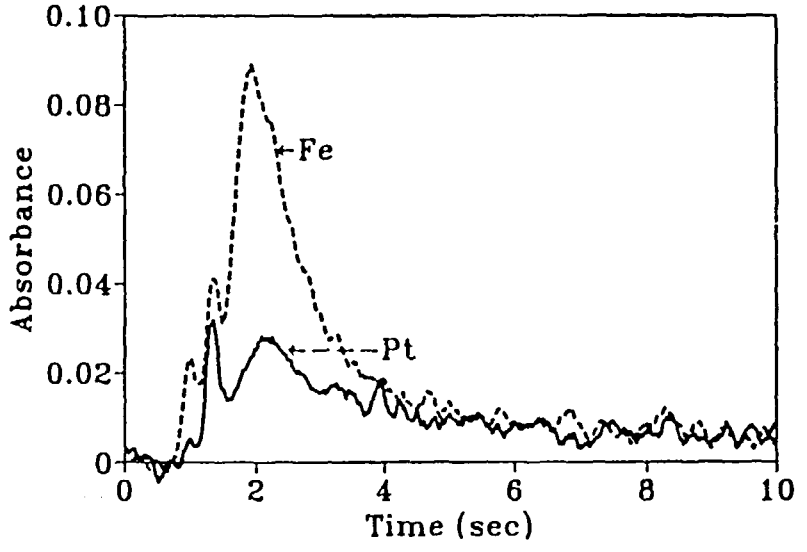

FIGURE 31. The Zeeman undercorrection error produced by Pt at the Fe line at 271.9 nm. The solid curve shows the Zeeman profile recorded for 40 ng of Pt alone using the conditions for Fe. (From Carnrick, G. R., Barnett, W., and Slavin, W., *Spectrochim. Acta*, 41B, 991, 1986. With permission.)

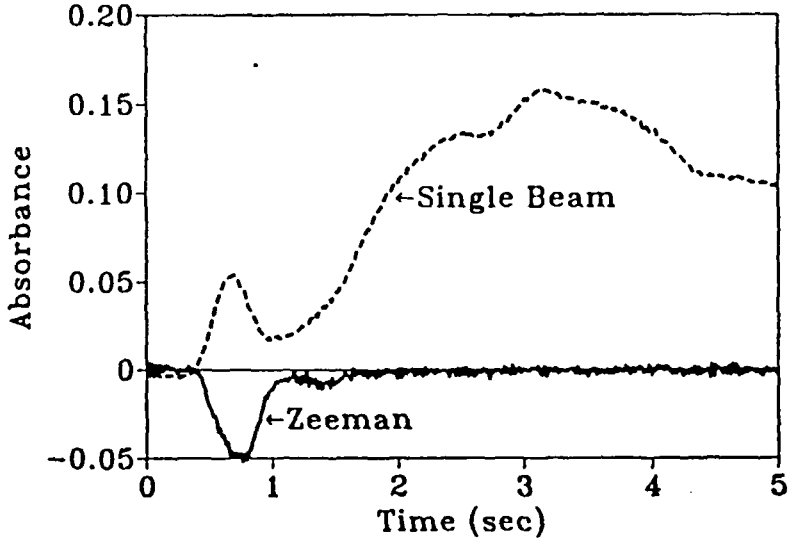

FIGURE 32. The Zeeman overcorrection error produced by phosphate using the Cd conditions at 326.1 nm. The dotted curve is the background signal. (From Carnrick, G. R., Barnett, W., and Slavin, W., *Spectrochim. Acta*, 41B, 991, 1986. With permission.)

result in an overcorrection, the presence of a PO molecular band is suggested which, while resolved from the 326.1-nm Cd line, exhibited molecular splitting as in Figure 27, panel A. Pearse and Gaydon[77] list a series of strong PO bands commencing at about 324 nm.

Thus, we have shown that errors may occur using Zeeman background correction from unresolved absorption lines or bands that exhibit Zeeman splitting. Problems may also occur if a sigma component from a nearby absorption line or molecular band is shifted to overlap the analyte absorption line during the magnet-on cycle. However, due to the extremely

Table 6
ZEEMAN INTERFERENCES (nm)

Analyte		Interferent		Δλ (nm)	Ref.
Ag	328.068	PO	—	—	74
Al	308.215	V	308.211	0.004	73
Au	267.595	Co	267.598	0.003	72
B	249.678	Co	249.671	0.007	72, 73
Bi	227.658	Co	227.653	0.005	73
Cd	326.106	PO	—	—	66
Co	243.666	Pt	243.669	0.003	73
Cr	260.533	Co	360.535	0.002	73
Eu	459.402	Cs	459.318[a]	—	73
Eu	459.402	V	459.411	0.009	73
Fe	271.902	Pt	271.904	0.002	65, 66
Ga	287.424	Fe	287.417	0.007	62
Hg	253.652	Co	253.649	0.003	65, 66, 72
Ni	341.477	Co	341.474	0.003	73
Ni	305.082	V	305.089	0.007	73
Pb	261.418	Co	261.413	0.005	73
Pd	247.642	Pb	247.638	0.004	73
Pt	265.945	Eu	265.942	0.003	73
Pt	306.471	Ni	306.462	0.009	73
Pt	273.396	Fe	273.400	0.004	73
Si	250.690	Co	250.688	0.002	73
Si	250.690	V	250.691	0.001	73
Sn	303.412	Cr	303.419	0.007	73
Sn	300.915	Ca	300.921	0.006	73
Zn	213.856	Fe	213.859	0.003	62

[a] From an Ar line at 459.324 nm.

narrow wavelength intervals, the probability of such overlaps is very small. With continuum correction, background correction errors are much more common because the background is measured over a wide spectral bandpass. The identified Zeeman errors are summarized in Table 6. Most of those listed are from Wibetoe and Langmyhr[73] for conditions that they specified. They studied in that paper the V and Cs interferences on Eu, showing that the Cs-Eu interference depends upon a nearby Ar line in Eu lamp which can be avoided with a narrow slit. Thus, most of the interferences in Table 6 referenced only to Reference 73 warrant additional study. Wibetoe and Langmyhr defined them as interferences if the test solution (free of analyte) provided a negative signal. Note also that most of those listed represent secondary lines of the analyte elements. Also, in some cases, preferred analytical conditions will avoid the interference. All of the interferences represent line separations <0.01 nm — most <0.004 nm. Those in the <0.004- or 0.003-nm category probably display direct line overlap and will be visible as interferences even when no background correction is used.

Overall, Zeeman background correction provides accurate correction for high background absorbances as well as for structured background. Considering the number of possible combinations of wavelengths, it is encouraging that so few cases have been found that produce errors. Overall, Zeeman background correction continues to provide accurate correction for high background absorbances as well as for structured background.

VIII. BACKGROUND CORRECTION TIMING ERRORS

Furnace absorbance peaks develop and dissipate very rapidly, as does the matrix back-

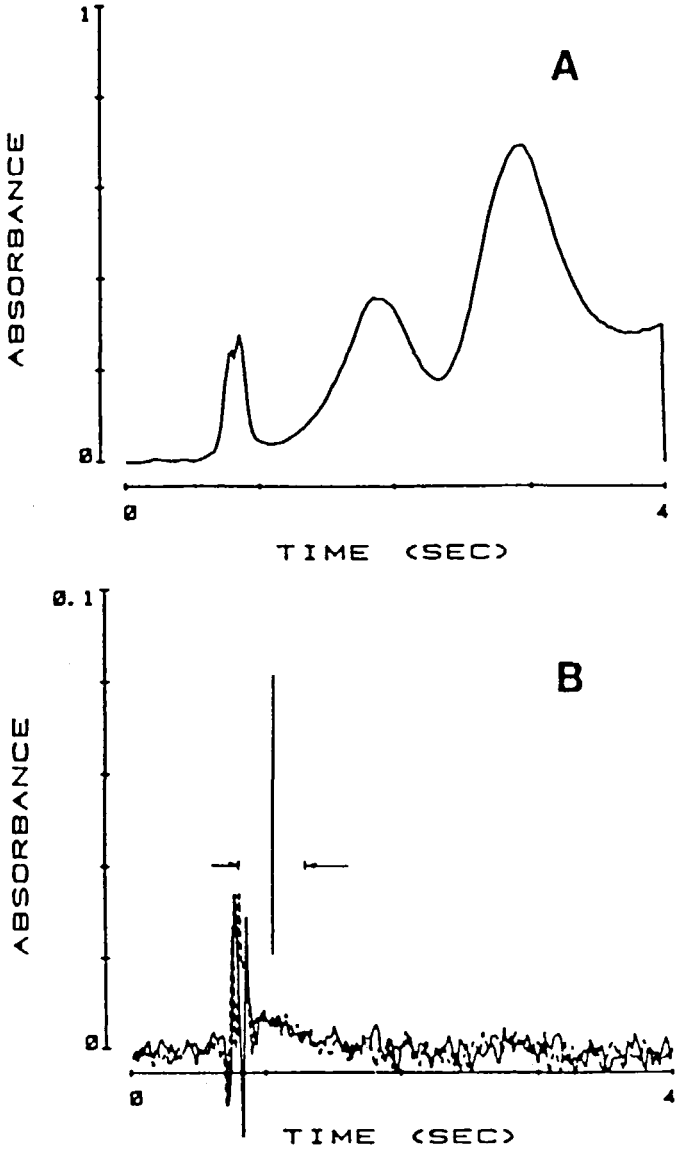

FIGURE 33. Disruption of the Zeeman-corrected signal for Cd (B) caused by the background illustrated in (A). The time that the Cd peak would be expected and its halfwidth are shown in (B). (From Slavin, W., Manning, D. C., Carnrick, G. R., and Pruszkowska, E., *Spectrochim. Acta*, 38B, 1157, 1983. With permission.)

ground. All the background correction techniques that are discussed here measure the AA and the background in sequence, albeit rapidly. When the background signal is used to correct the AA signal, it is usually assumed that the background at the time the AA signal was measured has not changed from when it was measured just before or after the AA signal. The numerous problems associated with continuum source correction systems masked this potential timing problem, but with Zeeman correction the problem arose and it has had to be dealt with.

Probably the first reported background timing problem is illustrated in Figures 33 and 34 from Reference 78. When the background changed very rapidly, its actual magnitude at the

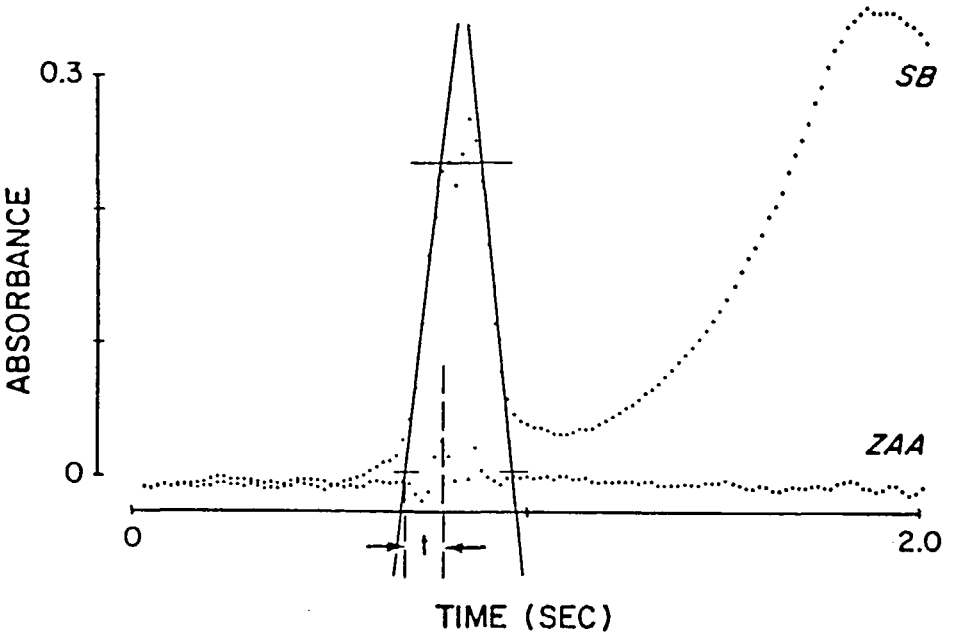

FIGURE 34. Replot of the first 2-sec data from Figure 33. Each 1-cycle data point is plotted. (From Slavin, W., Manning, D. C., Carnrick, G. R., and Pruszkowska, E., *Spectrochim. Acta*, 38B, 1157, 1983. With permission.)

moment that the AA signal was measured was in error, and this produced the erroneous Zeeman AAS signal shown in the figure. This has the effect of producing a derivative curve that first rises higher than it should and then falls lower than it should, as seen in the figure. To a first order, this problem has been corrected in modern instruments by measuring the background before and after measuring the AA and linearly interpolating the background to the time the AA signal was measured.[42]

The theory for this situation has been elegantly derived by Harnly and Holcombe.[79,80] Since background may not be changing linearly, the usual correction may not be adequate, and these authors considered higher-order errors and corrections. They showed experimentally some of these situations using a 2% NaCl solution near the Pb line at 283 nm. However, the practical significance of their work must be considered. There are several ways in which the magnitude of this error may be reduced in addition to making calculated corrections.

The furnace heating rate will control the rate at which the background signal is generated. As the heating rate is increased for other reasons, the magnitude of this signal-handling error will increase. However, instruments with faster heating rates should sample both the AA and background signal more rapidly, i.e., they should increase the chopping frequency, thus reducing the magnitude of the timing error.

Additionally, furnace AA signals should be integrated for quantitative purposes. The fact that the timing error is both positive and negative in the same run means that integration will average these peak variations. Even before we interpolated the background correction,[78] the quantitative effect of this timing error was very small because we integrated the signals. The Holcombe and Harnly[80] paper does not pay adequate attention to the influence of integration on this error.

IX. CONCLUSION

We must draw some conclusions in comparing the four background correction systems

discussed in this paper: (1) continuum source correction, (2) Zeeman correction, (3) continuum SIMAAC correction, and (4) S-H correction. The S-H technique is advantageous over continuum source (D_2) correction for certain elements because only a single source is required for both the AA and the background measurements. The SIMAAC technique provides excellent background correction, though not superior to Zeeman correction, but it provides some problems in the AA analyses. The signal-to-noise ratio is generally slightly (about twofold) poorer than conventional AAS for almost all metals, but it is much worse than that in the far UV. Arsenic and Se are impractical determinations by the SIMAAC technique and Zn and Cd have much degraded detection limits compared to the other AA techniques. This, and the expense of the high dispersion monochromator that is required, will probably limit the commercial attractiveness of the SIMAAC system. However, this system has certainly provided excellent analytical performance.

For flame AAS, the loss of analytical range compared to correction with a continuum source is an important limitation of the S-H system. This limitation on range seems to be an inherent part of the S-H technique. The loss of sensitivity of the S-H system will certainly be another limitation for flame AAS. The number of elements suffering loss of sensitivity may be reduced with additional attention to design parameters, but only at the expense of increased system complexity and/or loss of source intensity. The advantage of the S-H technique over continuum correction, in that more accurate correction can be made at high background, is not important in flame AAS since background is rarely large. Additionally, use of the high current pulse may reduce lamp life. The S-H technique may not be applicable with EDLs. Thus, we judge that continuum correction may continue to be preferred for flame AAS.

For furnace AAS, the range limitation of the S-H system is not so serious since the furnace is usually used only when high sensitivity is required. The fact that some elements cannot be used with the S-H technique and the loss of sensitivity represent serious problems for graphite furnace AAS. The atomic decay problem which limits the chopping frequency is probably the most serious limitation of the S-H technique. However, for some situations the S-H corrector will be better for furnace AAS than continuum correction.

Zeeman correction must be compared with the S-H system for the furnace. Certainly, an advantage of the S-H system is that it can be used for both flame and furnace, while Zeeman correction is more difficult to apply to flame AAS. The availability of the S-H system will probably increase the desirability of making instruments separately optimized for flame or furnace AAS. Probably the major disadvantage of the S-H technique compared to Zeeman correction is the long decay time required after the high current pulse, and this seems an inherent limitation. This long decay time produces two problems. First, it limits the frequency at which analyte and background signal can be sampled, making the system too "slow" for good furnace analyses. Second, the decay time reduces very greatly the duty cycle of the photometric system, thus degrading the signal-to-noise ratio available. This, together with the significantly greater reduction of sensitivity and of analytical range, compared to AC Zeeman correction, makes it less attractive than AC Zeeman correction for furnace AAS.

Thus, overall we judge that continuum correction is preferable over the S-H system for flame AAS and that the AC Zeeman system is preferable to the S-H system for furnace AAS. The technical material upon which the Zeeman technique is based is complex, but it is noteworthy that the instrumental operation is simple and the result is elegant. A single source serves both the analytical measurement and the background correction. The equipment is inherently inexpensive.

REFERENCES

1. **Slavin, W.,** *Atomic Absorption Spectroscopy,* Wiley Interscience, New York, 1968.
2. **Willis, J. B.,** *Anal. Chem.,* 34, 614, 1962.
3. **Koirtyohann, S. R. and Pickett, E. E.,** *Anal. Chem.,* 37, 601, 1965.
4. **Ling, C.,** *Anal. Chem.,* 39, 798, 1967.
5. **Barringer, A. R.,** *Inst. Min. Metall. Bull.,* 75B (714), 8120, 1966.
6. **Baranov, S. V., Grachev, B. D., Shikkeeva, I. A., and Zemskova, I. A.,** *J. Anal. Chem. (U.S.S.R.),* 37, 1756, 1982.
7. **Smith, S. B., Jr. and Hieftje, G. M.,** *Appl. Spectrosc.,* 37, 419, 1983.
8. **L'vov, B. V.,** *Inz. Fiz. Z.,* 2(2), 44, 1959; *Spectrochim. Acta,* 39B, 159, 1984.
9. **L'vov, B. V.,** *Spectrochim. Acta,* 17, 761, 1961.
10. **Massmann, H.,** *Spectrochim. Acta,* 23B, 215, 1968.
11. **Prügger, H. and Torge, R.,** U.S. Patent 3,676,004, 1972.
12. **Hadeishi, T. and McLaughlin, R. D.,** *Science,* 174, 404, 1971.
13. **Walsh, A.,** *Spectrochim. Acta,* 7, 108, 1955.
14. **Fassel, V. A., Mossotti, V. G., Grossman, W. E. L., and Kniseley, R. N.,** *Spectrochim. Acta,* 22, 347, 1966.
15. **O'Haver, T. C.,** *Analyst (London),* 109, 211, 1984.
16. **Snelleman, W.,** *Spectrochim. Acta,* 23B, 403, 1968.
17. **Svoboda, V.,** *Anal. Chem.,* 40, 1384, 1968.
18. **Kuhl, J., Marowsky, G., and Torge, R.,** *Anal. Chem.,* 44, 375, 1972.
19. **Schrenk, W. G., Meloan, C. E., and Frank, C. W.,** *Spectrosc. Lett.,* 1, 237, 1968.
20. **Bitter, F.,** *Appl. Opt.,* 1, 1, 1962.
21. **Alkemade, C. T. J. and Milatz, J. M. W.,** *J. Opt. Soc. Am.,* 45, 583, 1955.
22. **Tolansky, S.,** *High Resolution Spectroscopy,* Pitman, New York, 1947.
23. **Isaak, G. R.,** British Patents 918,878 and 918,879, 1963.
24. **Barnett, W. B., Vollmer, J. W., and De Nuzzo, S. M.,** *At. Absorpt. Newsl.,* 15, 33, 1976.
25. **Koizumi, H. and Yasuda, K.,** *Anal. Chem.,* 47, 1679, 1975.
26. **Stephens, R.,** U.S. Patent 3,893,768, 1975; **Stephens, R. and Ryan, D. E.,** *Talanta,* 22, 655, 1975.
27. **Parker, C. and Pearl, A.,** British Patent 1,385,791, 1975; U.S. Patent 4,341,470, 1982.
28. **Held, A. M.,** Thesis, Montana State University, Bozeman, 1972; **Woodriff, R.,** U.S. Patent 4,035,083, 1977.
29. **Uchida, Y. and Hattori, S.,** *Oyo Batsuri,* 44, 852, 1975.
30. **Dawson, J. B., Grassam, E., Ellis, D. J., and Keir, M. J.,** *Analyst (London),* 101, 315, 1976.
31. **Koizumi, H. and Yasuda, K.,** *Spectrochim. Acta,* 31B, 523, 1976.
32. **Hendrikx-Jongerius, C. and de Galan, L.,** *Anal. Chim. Acta,* 87, 259, 1976.
33. **de Loos-Vollebregt, M. T. C. and de Galan, L.,** *Spectrochim. Acta,* 33B, 495, 1978.
34. **Newstead, R. A., Price, W. J., and Whiteside, P. J.,** *Prog. Anal. At. Spectrosc.,* 1, 267, 1978.
35. **Welz, B.,** *Atomic Absorption Spectrometry,* V. C. H. Publishers, Weinheim, W. Germany, 1985.
36. **Slavin, W.,** *Graphite Furnace AAS, A Source Book,* Perkin-Elmer Corp., Norwalk, Conn., 1984.
37. **de Loos-Vollebregt, M. T. C. and de Galan, L.,** *Prog. Anal. At. Spectrosc.,* 8, 47, 1985.
38. **Yasuda, K., Koizumi, H., Ohishi, K., and Noda, T.,** *Prog. Anal. At. Spectrosc.,* 3, 299, 1980.
39. **Kahn, H. L.,** *At. Absorpt. Newsl.,* 7, 40, 1968.
40. **Massmann, H.,** *Ullmanns Encyklopädie der Technischen Chemie,* Band 5, 4th ed., Verlag Chemie, Weinheim, 1980, 423.
41. **Fernandez, F. J., Bohler, W., Beaty, M. M., and Barnett, W. B.,** *At. Spectrosc.,* 2, 73, 1981.
42. **Barnett, W. B., Bohler, W., Carnrick, G. R., and Slavin, W.,** *Spectrochim. Acta,* 40B, 1689, 1985.
43. *Techniques in Graphite Furnace AAS,* Perkin-Elmer Corp., Part No. 0993-8150, Norwalk, Conn., April 1985.
44. **L'vov, B. V., Nikolaev, V. G., Norman, E. A., Polzik, L. K., and Mojica, M.,** *Spectrochim. Acta,* 41B, 1043, 1986.
45. **Sotera, J. J. and Kahn, H. L.,** *Am. Lab.,* November 1982.
46. **de Galan, L. and de Loos-Vollebregt, M. T. C.,** *Spectrochim. Acta,* 39B, 1011, 1984.
47. **de Loos-Vollebregt, M. T. C. and de Galan, L.,** *Spectrochim. Acta,* 41B, 597, 1986.
48. **O'Haver, T. C. and Messman, J. D.,** *Prog. Anal. Spectrosc.,* 9, 483, 1986.
49. **Koizumi, H.,** *Anal. Chem.,* 50, 1101, 1978.
50. **Slavin, S. and Sattur, T.,** *At. Absorpt. Newsl.,* 7, 99, 1968.
51. **Manning, D. C.,** *At. Absorpt. Newsl.,* 17, 107, 1978.
52. **Vajda, F.,** *Anal. Chim. Acta,* 128, 31, 1981.
53. **Fernandez, F. J. and Giddings, R.,** *At. Spectrosc.,* 3, 61, 1982.

54. **Saeed, K. and Thomassen, Y.,** *Anal. Chim. Acta,* 130, 281, 1981.
55. **Welz, B. and Schlemmer, G.,** *J. Anal. At. Spectrom.,* 1, 119, 1986.
56. **Pruszkowska, E. and Barrett, P.,** *Spectrochim. Acta B,* 39, 485, 1984.
57. **Riley, K. W.,** *At. Spectrosc.,* 3, 120, 1982.
58. **Riley, K. W.,** *Analyst (London),* 109, 181, 1984.
59. **Fernandez, F. J. and Beaty, M. M.,** *Spectrochim. Acta,* 39B, 519, 1984.
60. **Carnrick, G. R., Manning, D. C., and Slavin, W.,** *Analyst (London),* 108, 1297, 1983.
61. **Welz, B., Völlkopf, U., and Grobenski, Z.,** *Anal. Chim. Acta,* 136, 201, 1982.
62. **Wibetoe, G. and Langmyhr, F. J.,** *Anal. Chim. Acta,* 165, 87, 1984.
63. **Slavin, W. and Manning, D. C.,** *Appl. Spectrosc.,* 37, 1, 1983.
64. **Völlkopf, U., Grobenski, Z., and Welz, B.,** *At. Spectrosc.,* 4, 165, 1983.
65. **Stephens, R. and Murphy, G. F.,** *Talanta,* 25, 441, 1978.
66. **Carnrick, G. R., Barnett, W., and Slavin, W.,** *Spectrochim. Acta,* 41B, 991, 1986.
67. **Dabeka, R. W.,** *Analyst (London),* 109, 1259, 1984.
68. **Andersen, J. R.,** *Analyst (London),* 110, 315, 1985.
69. **Siemer, D. D.,** *Anal. Chem.,* 56, 1519, 1984.
70. **Holcombe, J. A., Rayson, G. D., and Akerlind, N.,** *Spectrochim. Acta,* 37B, 319, 1982.
71. **Slavin, W., Carnrick, G. R., Manning, D. C., and Pruszkowska, E.,** *At. Spectrosc.,* 4, 69, 1983.
72. **Wibetoe, G. and Langmyhr, F. J.,** *Anal. Chim. Acta,* 176, 33, 1985.
73. **Wibetoe, G. and Langmyhr, F. J.,** *Anal. Chim. Acta,* 186, 155, 1986.
74. **Manning, D. C. and Slavin, W.,** *Spectrochim. Acta,* 42B, 755, 1987.
75. **Massmann, H.,** *Talanta,* 29, 1051, 1982.
76. **Carnrick, G. R., Lumas, B. K., and Barnett, W. B.,** *J. Anal. At. Spectrom.,* 1, 443, 1986.
77. **Pearse, R. W. B. and Gaydon, A. G.,** *Identification of Molecular Structure,* 2nd ed., Chapman and Hall, London, 1950.
78. **Slavin, W., Manning, D. C., Carnrick, G. R., and Pruszkowska, E.,** *Spectrochim. Acta,* 38B, 1157, 1983.
79. **Harnly, J. M. and Holcombe, J. A.,** *Anal. Chem.,* 57, 1983, 1985.
80. **Holcombe, J. A. and Harnly, J. M.,** *Anal. Chem.,* 58, 2606, 1986.